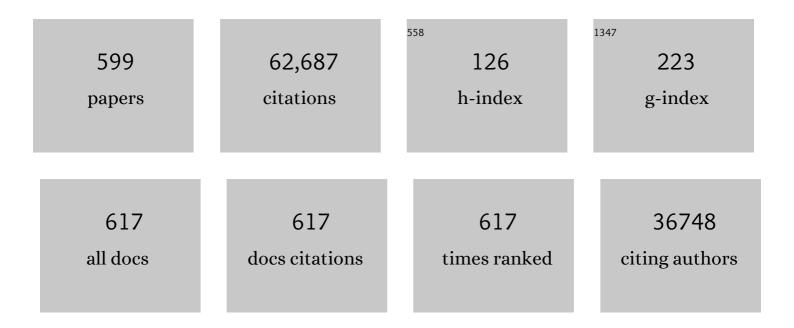
Dionysios D Dionysiou

List of Publications by Year in descending order

Source: https://exaly.com/author-pdf/5733781/publications.pdf Version: 2024-02-01



#	Article	IF	CITATIONS
1	A review on the visible light active titanium dioxide photocatalysts for environmental applications. Applied Catalysis B: Environmental, 2012, 125, 331-349.	20.2	3,320
2	Radical Generation by the Interaction of Transition Metals with Common Oxidants. Environmental Science & S	10.0	2,522
3	Degradation of Organic Contaminants in Water with Sulfate Radicals Generated by the Conjunction of Peroxymonosulfate with Cobalt. Environmental Science & Technology, 2003, 37, 4790-4797.	10.0	1,415
4	The use of zero-valent iron for groundwater remediation and wastewater treatment: A review. Journal of Hazardous Materials, 2014, 267, 194-205.	12.4	1,301
5	Sulfate radical-based ferrous–peroxymonosulfate oxidative system for PCBs degradation in aqueous and sediment systems. Applied Catalysis B: Environmental, 2009, 85, 171-179.	20.2	953
6	Cobalt-Mediated Activation of Peroxymonosulfate and Sulfate Radical Attack on Phenolic Compounds. Implications of Chloride Ions. Environmental Science & Technology, 2006, 40, 1000-1007.	10.0	802
7	Self-cleaning applications of TiO2 by photo-induced hydrophilicity and photocatalysis. Applied Catalysis B: Environmental, 2015, 176-177, 396-428.	20.2	739
8	Manipulation of Persistent Free Radicals in Biochar To Activate Persulfate for Contaminant Degradation. Environmental Science & Technology, 2015, 49, 5645-5653.	10.0	684
9	Activation of Persulfate by Quinones: Free Radical Reactions and Implication for the Degradation of PCBs. Environmental Science & amp; Technology, 2013, 47, 4605-4611.	10.0	673
10	Key Role of Persistent Free Radicals in Hydrogen Peroxide Activation by Biochar: Implications to Organic Contaminant Degradation. Environmental Science & Technology, 2014, 48, 1902-1910.	10.0	589
11	New Insights into the Mechanism of Visible Light Photocatalysis. Journal of Physical Chemistry Letters, 2014, 5, 2543-2554.	4.6	569
12	Degradation of microcystin-LR using sulfate radicals generated through photolysis, thermolysis and eâ~ transfer mechanisms. Applied Catalysis B: Environmental, 2010, 96, 290-298.	20.2	532
13	Transition metal/UV-based advanced oxidation technologies for water decontamination. Applied Catalysis B: Environmental, 2004, 54, 155-163.	20.2	528
14	Iron–cobalt mixed oxide nanocatalysts: Heterogeneous peroxymonosulfate activation, cobalt leaching, and ferromagnetic properties for environmental applications. Applied Catalysis B: Environmental, 2009, 88, 462-469.	20.2	526
15	Oxidative removal of Bisphenol A by UV-C/peroxymonosulfate (PMS): Kinetics, influence of co-existing chemicals and degradation pathway. Chemical Engineering Journal, 2015, 276, 193-204.	12.7	512
16	Opportunities and challenges in sustainable treatment and resource reuse of sewage sludge: A review. Chemical Engineering Journal, 2018, 337, 616-641.	12.7	510
17	The Technology Horizon for Photocatalytic Water Treatment: Sunrise or Sunset?. Environmental Science & Technology, 2019, 53, 2937-2947.	10.0	493
18	A review of solar and visible light active TiO2 photocatalysis for treating bacteria, cyanotoxins and contaminants of emerging concern. Materials Science in Semiconductor Processing, 2016, 42, 2-14.	4.0	484

#	Article	IF	CITATIONS
19	Heterogeneous Activation of Oxone Using Co3O4. Journal of Physical Chemistry B, 2005, 109, 13052-13055.	2.6	450
20	Sol–gel preparation of mesoporous photocatalytic TiO2 films and TiO2/Al2O3 composite membranes for environmental applications. Applied Catalysis B: Environmental, 2006, 63, 60-67.	20.2	449
21	Kinetic and mechanism investigation on the photochemical degradation of atrazine with activated H2O2, S2O82â^ and HSO5â^. Chemical Engineering Journal, 2014, 252, 393-403.	12.7	432
22	Superoxide radical driving the activation of persulfate by magnetite nanoparticles: Implications for the degradation of PCBs. Applied Catalysis B: Environmental, 2013, 129, 325-332.	20.2	420
23	Contamination Profiles of Perfluoroalkyl Substances (PFAS) in Groundwater in the Alluvial–Pluvial Plain of Hutuo River, China. Water (Switzerland), 2019, 11, 2316.	2.7	420
24	Heterogeneous Fenton catalysts: A review of recent advances. Journal of Hazardous Materials, 2021, 404, 124082.	12.4	412
25	Monodispersed CuFe2O4 nanoparticles anchored on natural kaolinite as highly efficient peroxymonosulfate catalyst for bisphenol A degradation. Applied Catalysis B: Environmental, 2019, 253, 206-217.	20.2	405
26	Size-Tunable Hydrothermal Synthesis of SnS ₂ Nanocrystals with High Performance in Visible Light-Driven Photocatalytic Reduction of Aqueous Cr(VI). Environmental Science & Technology, 2011, 45, 9324-9331.	10.0	389
27	Cr(VI) Adsorption and Reduction by Humic Acid Coated on Magnetite. Environmental Science & Technology, 2014, 48, 8078-8085.	10.0	378
28	2D Nanomaterials for Photocatalytic Hydrogen Production. ACS Energy Letters, 2019, 4, 1687-1709.	17.4	375
29	Phosphate adsorption using modified iron oxide-based sorbents in lake water: Kinetics, equilibrium, and column tests. Chemical Engineering Journal, 2016, 284, 1386-1396.	12.7	369
30	Visible light-assisted heterogeneous Fenton with ZnFe 2 O 4 for the degradation of Orange II in water. Applied Catalysis B: Environmental, 2016, 182, 456-468.	20.2	369
31	Effect of inorganic, synthetic and naturally occurring chelating agents on Fe(II) mediated advanced oxidation of chlorophenols. Water Research, 2009, 43, 684-694.	11.3	356
32	Sulfate radical-based degradation of polychlorinated biphenyls: Effects of chloride ion and reaction kinetics. Journal of Hazardous Materials, 2012, 227-228, 394-401.	12.4	356
33	Activation of peroxymonosulfate/persulfate by nanomaterials for sulfate radical-based advanced oxidation technologies. Current Opinion in Chemical Engineering, 2018, 19, 51-58.	7.8	352
34	Highly efficient activation of peroxymonosulfate by natural negatively-charged kaolinite with abundant hydroxyl groups for the degradation of atrazine. Applied Catalysis B: Environmental, 2019, 247, 10-23.	20.2	348
35	Innovative visible light-activated sulfur doped TiO2 films for water treatment. Applied Catalysis B: Environmental, 2011, 107, 77-87.	20.2	338
36	High-Performance Visible-Light-Driven SnS ₂ /SnO ₂ Nanocomposite Photocatalyst Prepared via In situ Hydrothermal Oxidation of SnS ₂ Nanoparticles. ACS Applied Materials & Interfaces, 2011, 3, 1528-1537.	8.0	321

#	Article	IF	CITATIONS
37	2D nanostructures for water purification: graphene and beyond. Nanoscale, 2016, 8, 15115-15131.	5.6	318
38	One-step hydrothermal synthesis of high-performance visible-light-driven SnS2/SnO2 nanoheterojunction photocatalyst for the reduction of aqueous Cr(VI). Applied Catalysis B: Environmental, 2014, 144, 730-738.	20.2	309
39	Mechanistic insight into reactivity of sulfate radical with aromatic contaminants through single-electron transfer pathway. Chemical Engineering Journal, 2017, 327, 1056-1065.	12.7	296
40	Mechanism of hydroxyl radical generation from biochar suspensions: Implications to diethyl phthalate degradation. Bioresource Technology, 2015, 176, 210-217.	9.6	284
41	Kinetics and mechanism investigation on the destruction of oxytetracycline by UV-254 nm activation of persulfate. Journal of Hazardous Materials, 2016, 305, 229-239.	12.4	284
42	Oxidative degradation of atrazine in aqueous solution by UV/H2O2/Fe2+, UV//Fe2+ and UV//Fe2+ processes: A comparative study. Chemical Engineering Journal, 2013, 218, 376-383.	12.7	282
43	Heterogeneous activation of peroxymonosulfate by supported cobalt catalysts for the degradation of 2,4-dichlorophenol in water: The effect of support, cobalt precursor, and UV radiation. Applied Catalysis B: Environmental, 2008, 77, 300-307.	20.2	281
44	Photocatalytic TiO2 films and membranes for the development of efficient wastewater treatment and reuse systems. Desalination, 2007, 202, 199-206.	8.2	276
45	Exceptional synergistic enhancement of the photocatalytic activity of SnS2 by coupling with polyaniline and N-doped reduced graphene oxide. Applied Catalysis B: Environmental, 2018, 236, 53-63.	20.2	274
46	Degradation kinetics and mechanism of oxytetracycline by hydroxyl radical-based advanced oxidation processes. Chemical Engineering Journal, 2016, 284, 1317-1327.	12.7	271
47	Novel fluorinated Bi 2 MoO 6 nanocrystals for efficient photocatalytic removal of water organic pollutants under different light source illumination. Applied Catalysis B: Environmental, 2017, 209, 1-11.	20.2	260
48	Highly efficient visible-light photocatalytic performance of Ag/AgIn5S8 for degradation of tetracycline hydrochloride and treatment of real pharmaceutical industry wastewater. Chemical Engineering Journal, 2018, 333, 423-433.	12.7	260
49	New insight into the mechanism of peroxymonosulfate activation by sulfur-containing minerals: Role of sulfur conversion in sulfate radical generation. Water Research, 2018, 142, 208-216.	11.3	254
50	Visible light-activated N-F-codoped TiO2 nanoparticles for the photocatalytic degradation of microcystin-LR in water. Catalysis Today, 2009, 144, 19-25.	4.4	253
51	Review and perspectives on the use of magnetic nanophotocatalysts (MNPCs) in water treatment. Chemical Engineering Journal, 2017, 310, 407-427.	12.7	247
52	Photogeneration of reactive oxygen species from biochar suspension for diethyl phthalate degradation. Applied Catalysis B: Environmental, 2017, 214, 34-45.	20.2	247
53	Efficient degradation of atrazine with porous sulfurized Fe2O3 as catalyst for peroxymonosulfate activation. Applied Catalysis B: Environmental, 2019, 259, 118056.	20.2	243
54	Efficient activation of peroxymonosulfate by magnetic Mn-MGO for degradation of bisphenol A. Journal of Hazardous Materials, 2016, 320, 150-159.	12.4	239

#	Article	IF	CITATIONS
55	Rapid toxicity elimination of organic pollutants by the photocatalysis of environment-friendly and magnetically recoverable step-scheme SnFe2O4/ZnFe2O4 nano-heterojunctions. Chemical Engineering Journal, 2020, 379, 122264.	12.7	238
56	Degradation kinetics and mechanism of β-lactam antibiotics by the activation of H2O2 and Na2S2O8 under UV-254nm irradiation. Journal of Hazardous Materials, 2014, 279, 375-383.	12.4	236
57	Significant role of UV and carbonate radical on the degradation of oxytetracycline in UV-AOPs: Kinetics and mechanism. Water Research, 2016, 95, 195-204.	11.3	234
58	Nanocrystalline cobalt oxide immobilized on titanium dioxide nanoparticles for the heterogeneous activation of peroxymonosulfate. Applied Catalysis B: Environmental, 2007, 74, 170-178.	20.2	233
59	Mesoporous Nitrogen-Doped TiO ₂ for the Photocatalytic Destruction of the Cyanobacterial Toxin Microcystin-LR under Visible Light Irradiation. Environmental Science & Technology, 2007, 41, 7530-7535.	10.0	232
60	Synthesis of Reactive Nano-Fe/Pd Bimetallic System-Impregnated Activated Carbon for the Simultaneous Adsorption and Dechlorination of PCBs. Chemistry of Materials, 2008, 20, 3649-3655.	6.7	232
61	Facile preparation of porous Mn/Fe3O4 cubes as peroxymonosulfate activating catalyst for effective bisphenol A degradation. Chemical Engineering Journal, 2019, 376, 119193.	12.7	231
62	Toxic cyanobacteria and drinking water: Impacts, detection, and treatment. Harmful Algae, 2016, 54, 174-193.	4.8	229
63	Destruction of cyanobacterial toxin cylindrospermopsin by hydroxyl radicals and sulfate radicals using UV-254nm activation of hydrogen peroxide, persulfate and peroxymonosulfate. Journal of Photochemistry and Photobiology A: Chemistry, 2013, 251, 160-166.	3.9	224
64	Role of pH on photolytic and photocatalytic degradation of antibiotic oxytetracycline in aqueous solution under visible/solar light: Kinetics and mechanism studies. Applied Catalysis B: Environmental, 2013, 134-135, 83-92.	20.2	214
65	What is the role of light in persulfate-based advanced oxidation for water treatment?. Water Research, 2021, 189, 116627.	11.3	214
66	Degradation of atrazine by ZnxCu1â^'xFe2O4 nanomaterial-catalyzed sulfite under UV–vis light irradiation: Green strategy to generate SO4â". Applied Catalysis B: Environmental, 2018, 221, 380-392.	20.2	212
67	Electrochemical activation of peroxymonosulfate with ACF cathode: Kinetics, influencing factors, mechanism, and application potential. Water Research, 2019, 159, 111-121.	11.3	212
68	Microplastics as Both a Sink and a Source of Bisphenol A in the Marine Environment. Environmental Science & Technology, 2019, 53, 10188-10196.	10.0	211
69	Efficient removal of microcystin-LR by UV-C/H2O2 in synthetic and natural water samples. Water Research, 2012, 46, 1501-1510.	11.3	206
70	Efficient removal of endosulfan from aqueous solution by UV-C/peroxides: A comparative study. Journal of Hazardous Materials, 2013, 263, 584-592.	12.4	206
71	Intermediates and Reaction Pathways from the Degradation of Microcystin-LR with Sulfate Radicals. Environmental Science & Technology, 2010, 44, 7238-7244.	10.0	205
72	Trichloroethene Hydrodechlorination in Water by Highly Disordered Monometallic Nanoiron. Chemistry of Materials, 2005, 17, 5315-5322.	6.7	204

#	Article	IF	CITATIONS
73	Visible-light-responsive graphene-functionalized Bi-bridge Z-scheme black BiOCl/Bi2O3 heterojunction with oxygen vacancy and multiple charge transfer channels for efficient photocatalytic degradation of 2-nitrophenol and industrial wastewater treatment. Applied Catalysis B: Environmental, 2018, 238, 61-69.	20.2	203
74	Aligned α-FeOOH nanorods anchored on a graphene oxide-carbon nanotubes aerogel can serve as an effective Fenton-like oxidation catalyst. Applied Catalysis B: Environmental, 2017, 213, 74-86.	20.2	202
75	Visible light-sensitized S, N and C co-doped polymorphic TiO2 for photocatalytic destruction of microcystin-LR. Applied Catalysis B: Environmental, 2014, 144, 614-621.	20.2	197
76	Kinetics and mechanism of sulfate radical- and hydroxyl radical-induced degradation of highly chlorinated pesticide lindane in UV/peroxymonosulfate system. Chemical Engineering Journal, 2017, 318, 135-142.	12.7	196
77	Photochemical degradation of oxytetracycline: Influence of pH and role of carbonate radical. Chemical Engineering Journal, 2015, 276, 113-121.	12.7	194
78	Natural illite-based ultrafine cobalt oxide with abundant oxygen-vacancies for highly efficient Fenton-like catalysis. Applied Catalysis B: Environmental, 2020, 261, 118214.	20.2	194
79	HNO3-involved one-step low temperature solvothermal synthesis of N-doped TiO2 nanocrystals for efficient photocatalytic reduction of Cr(VI) in water. Applied Catalysis B: Environmental, 2013, 142-143, 249-258.	20.2	190
80	Chemical and microbial decontamination of pool water using activated potassium peroxymonosulfate. Water Research, 2008, 42, 2899-2910.	11.3	189
81	Antibacterial properties of F-doped ZnO visible light photocatalyst. Journal of Hazardous Materials, 2017, 324, 39-47.	12.4	187
82	Hetero-nanostructured metal oxide-based hybrid photocatalysts for enhanced photoelectrochemical water splitting – A review. International Journal of Hydrogen Energy, 2020, 45, 18331-18347.	7.1	185
83	Efficient transformation of DDTs with Persulfate Activation by Zero-valent Iron Nanoparticles: A Mechanistic Study. Journal of Hazardous Materials, 2016, 316, 232-241.	12.4	181
84	Destruction of microcystins by conventional and advanced oxidation processes: A review. Separation and Purification Technology, 2012, 91, 3-17.	7.9	180
85	Design and fabrication of microsphere photocatalysts for environmental purification and energy conversion. Chemical Engineering Journal, 2016, 287, 117-129.	12.7	180
86	The facile fabrication of novel visible-light-driven Z-scheme CuInS2/Bi2WO6 heterojunction with intimate interface contact by in situ hydrothermal growth strategy for extraordinary photocatalytic performance. Chemical Engineering Journal, 2019, 356, 819-829.	12.7	177
87	Activation of persulfate with vanadium species for PCBs degradation: A mechanistic study. Applied Catalysis B: Environmental, 2017, 202, 1-11.	20.2	175
88	Novel visible-light-driven direct Z-scheme CdS/CuInS2 nanoplates for excellent photocatalytic degradation performance and highly-efficient Cr(VI) reduction. Chemical Engineering Journal, 2019, 361, 1451-1461.	12.7	171
89	Oxidative removal of brilliant green by UV/S2O82‒, UV/HSO5‒ and UV/H2O2 processes in aqueous media: A comparative study. Journal of Hazardous Materials, 2018, 357, 506-514.	12.4	170
90	Nanomedicine: An effective tool in cancer therapy. International Journal of Pharmaceutics, 2018, 540, 132-149.	5.2	169

#	Article	IF	CITATIONS
91	Synthesis, structural characterization and evaluation of sol–gel-based NF-TiO2 films with visible light-photoactivation for the removal of microcystin-LRâ~†. Applied Catalysis B: Environmental, 2010, 99, 378-387.	20.2	168
92	Thermally Stable Nanocrystalline TiO2Photocatalysts Synthesized via Solâ^'Gel Methods Modified with Ionic Liquid and Surfactant Molecules. Chemistry of Materials, 2006, 18, 5377-5384.	6.7	166
93	Solar photocatalysis for water disinfection: materials and reactor design. Catalysis Science and Technology, 2014, 4, 1211-1226.	4.1	165
94	Assessment of the roles of reactive oxygen species in the UV and visible light photocatalytic degradation of cyanotoxins and water taste and odor compounds using C–TiO2. Water Research, 2016, 90, 52-61.	11.3	165
95	Synthesis of GO/TiO2/Bi2WO6 nanocomposites with enhanced visible light photocatalytic degradation of ethylene. Applied Catalysis B: Environmental, 2019, 246, 303-311.	20.2	165
96	Unveiling New Degradation Intermediates/Pathways from the Photocatalytic Degradation of Microcystin-LR. Environmental Science & amp; Technology, 2008, 42, 8877-8883.	10.0	163
97	Continuous-mode photocatalytic degradation of chlorinated phenols and pesticides in water using a bench-scale TiO2 rotating disk reactor. Applied Catalysis B: Environmental, 2000, 24, 139-155.	20.2	160
98	Kinetic and mechanistic aspects of hydroxyl radical‒mediated degradation of naproxen and reaction intermediates. Water Research, 2018, 137, 233-241.	11.3	160
99	Use of selected scavengers for the determination of NF-TiO2 reactive oxygen species during the degradation of microcystin-LR under visible light irradiation. Journal of Molecular Catalysis A, 2016, 425, 183-189.	4.8	157
100	Development of a new efficient visible-light-driven photocatalyst from SnS2 and polyvinyl chloride. Journal of Catalysis, 2016, 344, 692-700.	6.2	157
101	Recent advances in flue gas desulfurization gypsum processes and applications – A review. Journal of Environmental Management, 2019, 251, 109572.	7.8	157
102	Cobalt ferrite nanoparticles with controlled composition-peroxymonosulfate mediated degradation of 2-phenylbenzimidazole-5-sulfonic acid. Applied Catalysis B: Environmental, 2018, 221, 266-279.	20.2	155
103	Highly efficient Sr/Ce/activated carbon bimetallic nanocomposite for photoinduced degradation of rhodamine B. Catalysis Today, 2019, 335, 437-451.	4.4	155
104	TiO2 photocatalytic films on stainless steel: The role of Degussa P-25 in modified sol–gel methods. Applied Catalysis B: Environmental, 2006, 62, 255-264.	20.2	152
105	A path to clean water. Science, 2018, 361, 222-224.	12.6	151
106	Degradation and transformation of bisphenol A in UV/Sodium percarbonate: Dual role of carbonate radical anion. Water Research, 2020, 171, 115394.	11.3	151
107	Construction of novel symmetric double Z-scheme BiFeO3/CuBi2O4/BaTiO3 photocatalyst with enhanced solar-light-driven photocatalytic performance for degradation of norfloxacin. Applied Catalysis B: Environmental, 2020, 272, 119017.	20.2	150
108	Advanced Oxidation Processes for Water Treatment. Journal of Physical Chemistry Letters, 2012, 3, 2112-2113.	4.6	148

#	Article	IF	CITATIONS
109	Contribution of alcohol radicals to contaminant degradation in quenching studies of persulfate activation process. Water Research, 2018, 139, 66-73.	11.3	148
110	A review on cylindrospermopsin: the global occurrence, detection, toxicity and degradation of a potent cyanotoxin. Environmental Sciences: Processes and Impacts, 2013, 15, 1979.	3.5	147
111	Plasmonic-based nanomaterials for environmental remediation. Applied Catalysis B: Environmental, 2018, 237, 721-741.	20.2	146
112	TiO2 photocatalyst for indoor air remediation: Influence of crystallinity, crystal phase, and UV radiation intensity on trichloroethylene degradation. Applied Catalysis B: Environmental, 2010, 94, 211-218.	20.2	145
113	Solar photocatalytic disinfection of water using titanium dioxide graphene composites. Chemical Engineering Journal, 2015, 261, 36-44.	12.7	145
114	Micelles as Soil and Water Decontamination Agents. Chemical Reviews, 2016, 116, 6042-6074.	47.7	144
115	Hydrothermal synthesis of photoactive nitrogen- and boron- codoped TiO2 nanoparticles for the treatment of bisphenol A in wastewater: Synthesis, photocatalytic activity, degradation byproducts and reaction pathways. Applied Catalysis B: Environmental, 2019, 241, 598-611.	20.2	142
116	Transformation of polychlorinated biphenyls by persulfate at ambient temperature. Chemosphere, 2013, 90, 1573-1580.	8.2	140
117	Photochemical treatment of tyrosol, a model phenolic compound present in olive mill wastewater, by hydroxyl and sulfate radical-based advanced oxidation processes (AOPs). Journal of Hazardous Materials, 2019, 367, 734-742.	12.4	139
118	Kinetics and mechanisms of cylindrospermopsin destruction by sulfate radical-based advanced oxidation processes. Water Research, 2014, 63, 168-178.	11.3	138
119	High performance sulfur, nitrogen and carbon doped mesoporous anatase–brookite TiO2 photocatalyst for the removal of microcystin-LR under visible light irradiation. Journal of Hazardous Materials, 2014, 280, 723-733.	12.4	138
120	Metal-mediated oxidation of fluoroquinolone antibiotics in water: A review on kinetics, transformation products, and toxicity assessment. Journal of Hazardous Materials, 2018, 344, 1136-1154.	12.4	138
121	Sulfamethoxazole degradation by visible light assisted peroxymonosulfate process based on nanohybrid manganese dioxide incorporating ferric oxide. Applied Catalysis B: Environmental, 2020, 278, 119297.	20.2	138
122	Roles of oxygen-containing functional groups of O-doped g-C3N4 in catalytic ozonation: Quantitative relationship and first-principles investigation. Applied Catalysis B: Environmental, 2021, 292, 120155.	20.2	137
123	Adsorption, oxidation, and reduction behavior of arsenic in the removal of aqueous As(III) by mesoporous Fe/Al bimetallic particles. Water Research, 2016, 96, 22-31.	11.3	135
124	Rapid removal of tetrabromobisphenol A by α-Fe2O3-x@Graphene@Montmorillonite catalyst with oxygen vacancies through peroxymonosulfate activation: Role of halogen and α-hydroxyalkyl radicals. Applied Catalysis B: Environmental, 2020, 260, 118129.	20.2	135
125	Microwave degradation of methyl orange dye in aqueous solution in the presence of nano-TiO2-supported activated carbon (supported-TiO2/AC/MW). Journal of Hazardous Materials, 2012, 209-210, 271-277.	12.4	134
126	Photocatalytic removal of atrazine using N-doped TiO2 supported on phosphors. Applied Catalysis B: Environmental, 2015, 164, 462-474.	20.2	134

#	Article	IF	CITATIONS
127	Effects of water parameters on the degradation of microcystin-LR under visible light-activated TiO2 photocatalyst. Water Research, 2011, 45, 3787-3796.	11.3	131
128	Correlation of structural properties and film thickness to photocatalytic activity of thick TiO2 films coated on stainless steel. Applied Catalysis B: Environmental, 2006, 69, 24-33.	20.2	130
129	Photoinactivation of <i>Escherichia coli</i> by Sulfur-Doped and Nitrogen–Fluorine-Codoped TiO ₂ Nanoparticles under Solar Simulated Light and Visible Light Irradiation. Environmental Science & Technology, 2013, 47, 9988-9996.	10.0	129
130	Effects of HCO ₃ [–] on Degradation of Toxic Contaminants of Emerging Concern by UV/NO ₃ [–] . Environmental Science & Technology, 2018, 52, 12697-12707.	10.0	129
131	Diatomite supported hierarchical 2D CoNi3O4 nanoribbons as highly efficient peroxymonosulfate catalyst for atrazine degradation. Applied Catalysis B: Environmental, 2020, 272, 118971.	20.2	129
132	Synthesis of nanocrystalline photocatalytic TiO2 thin films and particles using sol–gel method modified with nonionic surfactants. Thin Solid Films, 2006, 510, 107-114.	1.8	128
133	LC/MS/MS structure elucidation of reaction intermediates formed during the TiO2 photocatalysis of microcystin-LR. Toxicon, 2008, 51, 1103-1118.	1.6	128
134	Superoxide mediated production of hydroxyl radicals by magnetite nanoparticles: Demonstration in the degradation of 2-chlorobiphenyl. Journal of Hazardous Materials, 2013, 250-251, 68-75.	12.4	126
135	Understanding Mechanisms of Synergy between Acidification and Ultrasound Treatments for Activated Sludge Dewatering: From Bench to Pilot–Scale Investigation. Environmental Science & Technology, 2018, 52, 4313-4323.	10.0	126
136	Enhancement of the Cr(VI) adsorption and photocatalytic reduction activity of g-C3N4 by hydrothermal treatment in HNO3 aqueous solution. Applied Catalysis A: General, 2016, 521, 9-18.	4.3	123
137	lonic liquid assisted preparation of nanostructured TiO2 particles. Chemical Communications, 2004, , 2000.	4.1	122
138	Distribution and bioaccumulation of steroidal and phenolic endocrine disrupting chemicals in wild fish species from Dianchi Lake, China. Environmental Pollution, 2011, 159, 2815-2822.	7.5	122
139	Optimization of photocatalytic performance of TiO2 coated glass microspheres using response surface methodology and the application for degradation of dimethyl phthalate. Journal of Photochemistry and Photobiology A: Chemistry, 2013, 262, 7-13.	3.9	122
140	Preparation and antibacterial properties of gold nanoparticles: a review. Environmental Chemistry Letters, 2021, 19, 167-187.	16.2	121
141	Degradation of 2,4-dichlorophenoxyacetic acid (2,4-D) using cobalt-peroxymonosulfate in Fenton-like process. Journal of Photochemistry and Photobiology A: Chemistry, 2007, 186, 357-363.	3.9	119
142	Diffused sunlight driven highly synergistic pathway for complete mineralization of organic contaminants using reduced graphene oxide supported photocatalyst. Journal of Hazardous Materials, 2015, 291, 83-92.	12.4	119
143	Removal of carbamazepine in water by electro-activated carbon fiber-peroxydisulfate: Comparison, optimization, recycle, and mechanism study. Chemical Engineering Journal, 2018, 343, 28-36.	12.7	119
144	Chlorate Formation Mechanism in the Presence of Sulfate Radical, Chloride, Bromide and Natural Organic Matter. Environmental Science & Technology, 2018, 52, 6317-6325.	10.0	119

#	Article	IF	CITATIONS
145	Oxidative dehydrogenation of ethane: catalytic and mechanistic aspects and future trends. Chemical Society Reviews, 2021, 50, 4564-4605.	38.1	119
146	Adsorption and photocatalytic degradation of aromatic organoarsenic compounds in TiO2 suspension. Catalysis Today, 2014, 224, 83-88.	4.4	118
147	Inactivation of pathogenic microorganisms by sulfate radical: Present and future. Chemical Engineering Journal, 2019, 371, 222-232.	12.7	118
148	Mechanistic insight into degradation of endocrine disrupting chemical by hydroxyl radical: An experimental and theoretical approach. Environmental Pollution, 2017, 231, 1446-1452.	7.5	117
149	Insight into carbamazepine degradation by UV/monochloramine: Reaction mechanism, oxidation products, and DBPs formation. Water Research, 2018, 146, 288-297.	11.3	117
150	Magnetically recoverable MgFe2O4/conjugated polyvinyl chloride derivative nanocomposite with higher visible-light photocatalytic activity for treating Cr(VI)-polluted water. Separation and Purification Technology, 2020, 236, 116272.	7.9	116
151	Limitations and prospects of sulfate-radical based advanced oxidation processes. Journal of Environmental Chemical Engineering, 2020, 8, 103849.	6.7	116
152	Novel hierarchical carbon quantum dots-decorated BiOCl nanosheet/carbonized eggshell membrane composites for improved removal of organic contaminants from water via synergistic adsorption and photocatalysis. Chemical Engineering Journal, 2021, 420, 129582.	12.7	116
153	A comparative study on physicochemical properties and photocatalytic behavior of macroporous TiO2-P25 composite films and macroporous TiO2 films coated on stainless steel substrate. Applied Catalysis A: General, 2007, 317, 129-137.	4.3	115
154	Copper modified-TiO2 catalysts for hydrogen generation through photoreforming of organics. A short review. International Journal of Hydrogen Energy, 2014, 39, 16812-16831.	7.1	115
155	Chemical structure-based predictive model for the oxidation of trace organic contaminants by sulfate radical. Water Research, 2017, 116, 106-115.	11.3	114
156	UV direct photolysis of sulfamethoxazole and ibuprofen: An experimental and modelling study. Journal of Hazardous Materials, 2018, 343, 132-139.	12.4	114
157	Diclofenac removal by simulated solar assisted photocatalysis using TiO2-based zeolite catalyst; mechanisms, pathways and environmental aspects. Chemical Engineering Journal, 2016, 304, 289-302.	12.7	113
158	A new high efficiency visible-light photocatalyst made of SnS2 and conjugated derivative of polyvinyl alcohol and its application to Cr(VI) reduction. Chemical Engineering Journal, 2017, 324, 140-153.	12.7	113
159	UV and visible light activated TiO2 photocatalysis of 6-hydroxymethyl uracil, a model compound for the potent cyanotoxin cylindrospermopsin. Catalysis Today, 2014, 224, 70-76.	4.4	112
160	Advances in catalytic/photocatalytic bacterial inactivation by nano Ag and Cu coated surfaces and medical devices. Applied Catalysis B: Environmental, 2019, 240, 291-318.	20.2	112
161	Efficient toxicity elimination of aqueous Cr(VI) by positively-charged BiOClxI1-x, BiOBrxI1-x and BiOClxBr1-x solid solution with internal hole-scavenging capacity via the synergy of adsorption and photocatalytic reduction. Journal of Hazardous Materials, 2020, 383, 121127.	12.4	111
162	Quantitative structure–activity relationships for reactivities of sulfate and hydroxyl radicals with aromatic contaminants through single–electron transfer pathway. Journal of Hazardous Materials, 2018, 344, 1165-1173.	12.4	109

#	Article	IF	CITATIONS
163	Mechanisms of Interaction between Persulfate and Soil Constituents: Activation, Free Radical Formation, Conversion, and Identification. Environmental Science & Technology, 2018, 52, 14352-14361.	10.0	109
164	Novel magnetic rod-like Mn-Fe oxycarbide toward peroxymonosulfate activation for efficient oxidation of butyl paraben: Radical oxidation versus singlet oxygenation. Applied Catalysis B: Environmental, 2020, 268, 118549.	20.2	108
165	Effect of key parameters on the photocatalytic oxidation of toluene at low concentrations in air under 254+185nm UV irradiation. Applied Catalysis B: Environmental, 2010, 95, 312-319.	20.2	107
166	Occurrence, removal and bioaccumulation of steroid estrogens in Dianchi Lake catchment, China. Environment International, 2013, 59, 262-273.	10.0	107
167	Reductive and oxidative degradation of iopamidol, iodinated X-ray contrast media, by Fe(III)-oxalate under UV and visible light treatment. Water Research, 2014, 67, 144-153.	11.3	107
168	Synthesis of eosin modified TiO2 film with co-exposed {001} and {101} facets for photocatalytic degradation of para-aminobenzoic acid and solar H2 production. Applied Catalysis B: Environmental, 2020, 265, 118557.	20.2	106
169	Cyanotoxins: New Generation of Water Contaminants. Journal of Environmental Engineering, ASCE, 2005, 131, 1239-1243.	1.4	105
170	Bromate formation in bromide-containing water through the cobalt-mediated activation of peroxymonosulfate. Water Research, 2015, 83, 132-140.	11.3	103
171	Synthesis of BiVO4/P25 composites for the photocatalytic degradation of ethylene under visible light. Chemical Engineering Journal, 2017, 314, 443-452.	12.7	103
172	Flowing nitrogen atmosphere induced rich oxygen vacancies overspread the surface of TiO2/kaolinite composite for enhanced photocatalytic activity within broad radiation spectrum. Applied Catalysis B: Environmental, 2018, 236, 76-87.	20.2	103
173	Enhancing the Fenton-like Catalytic Activity of nFe ₂ O ₃ by MIL-53(Cu) Support: A Mechanistic Investigation. Environmental Science & Technology, 2020, 54, 5258-5267.	10.0	103
174	Construction of novel Z-scheme Ag/FeTiO3/Ag/BiFeO3 photocatalyst with enhanced visible-light-driven photocatalytic performance for degradation of norfloxacin. Chemical Engineering Journal, 2018, 351, 1056-1066.	12.7	102
175	Efficient degradation of bisphenol A in water by heterogeneous activation of peroxymonosulfate using highly active cobalt ferrite nanoparticles. Journal of Hazardous Materials, 2020, 399, 122979.	12.4	102
176	Fe/Al bimetallic particles for the fast and highly efficient removal of Cr(VI) over a wide pH range: Performance and mechanism. Journal of Hazardous Materials, 2015, 298, 261-269.	12.4	101
177	Hydroxyl Radical Oxidation of Cylindrospermopsin (Cyanobacterial Toxin) and Its Role in the Photochemical Transformation. Environmental Science & Technology, 2012, 46, 12608-12615.	10.0	98
178	Oxidation of Microcystin-LR by Ferrate(VI): Kinetics, Degradation Pathways, and Toxicity Assessments. Environmental Science & Technology, 2014, 48, 12164-12172.	10.0	98
179	Degradation kinetics and mechanism of desethyl-atrazine and desisopropyl-atrazine in water with OH and SO4â^' based-AOPs. Chemical Engineering Journal, 2017, 325, 485-494.	12.7	98
180	Impact of the morphological properties of thin TiO2 photocatalytic films on the detoxification of water contaminated with the cyanotoxin, microcystin-LR. Applied Catalysis B: Environmental, 2009, 91, 165-173.	20.2	97

#	Article	IF	CITATIONS
181	Enhanced antibiotic removal through a dual-reaction-center Fenton-like process in 3D graphene based hydrogels. Environmental Science: Nano, 2019, 6, 388-398.	4.3	96
182	Prototype composite membranes of partially reduced graphene oxide/TiO2 for photocatalytic ultrafiltration water treatment under visible light. Applied Catalysis B: Environmental, 2014, 158-159, 361-372.	20.2	95
183	Malic acid-enhanced chitosan hydrogel beads (mCHBs) for the removal of Cr(VI) and Cu(II) from aqueous solution. Chemical Engineering Journal, 2018, 353, 225-236.	12.7	94
184	Efficient transformation and elimination of roxarsone and its metabolites by a new α-FeOOH@GCA activating persulfate system under UV irradiation with subsequent As(V) recovery. Applied Catalysis B: Environmental, 2019, 245, 207-219.	20.2	93
185	The band structure control of visible-light-driven rGO/ZnS-MoS2 for excellent photocatalytic degradation performance and long-term stability. Chemical Engineering Journal, 2018, 350, 248-256.	12.7	92
186	A Comprehensive Review: Development of Electrochemical Biosensors for Detection of Cyanotoxins in Freshwater. ACS Sensors, 2019, 4, 1151-1173.	7.8	92
187	The effect of basic pH and carbonate ion on the mechanism of photocatalytic destruction of cylindrospermopsin. Water Research, 2015, 73, 353-361.	11.3	91
188	Tertiary treatment of landfill leachate by an integrated Electro-Oxidation/Electro-Coagulation/Electro-Reduction process: Performance and mechanism. Journal of Hazardous Materials, 2018, 351, 90-97.	12.4	91
189	A review on the degradation efficiency, DBP formation, and toxicity variation in the UV/chlorine treatment of micropollutants. Chemical Engineering Journal, 2021, 424, 130053.	12.7	91
190	Synergy between Iron and Selenide on FeSe ₂ (111) Surface Driving Peroxymonosulfate Activation for Efficient Degradation of Pollutants. Environmental Science & Technology, 2020, 54, 15489-15498.	10.0	90
191	Degradation of 1,4-dioxane from industrial wastewater by solar photocatalysis using immobilized NF-TiO2 composite with monodisperse TiO2 nanoparticles. Applied Catalysis B: Environmental, 2016, 180, 44-52.	20.2	89
192	Destruction of microcystins (cyanotoxins) by UV-254Ânm-based direct photolysis and advanced oxidation processes (AOPs): Influence of variable amino acids on the degradation kinetics and reaction mechanisms. Water Research, 2015, 74, 227-238.	11.3	88
193	Influence of mesoporous defect induced mixed-valent NiO (Ni2+/Ni3+)-TiO2 nanocomposite for non-enzymatic glucose biosensors. Sensors and Actuators B: Chemical, 2018, 264, 27-37.	7.8	88
194	A Multiwalledâ€Carbonâ€Nanotubeâ€Based Biosensor for Monitoring Microcystinâ€LR in Sources of Drinking Water Supplies. Advanced Functional Materials, 2013, 23, 1807-1816.	14.9	87
195	Fabrication of ternary reduced graphene oxide/SnS 2 /ZnFe 2 O 4 composite for high visible-light photocatalytic activity and stability. Journal of Hazardous Materials, 2017, 332, 149-161.	12.4	87
196	Enhanced photocatalytic CO2 reduction via the synergistic effect between Ag and activated carbon in TiO2/AC-Ag ternary composite. Chemical Engineering Journal, 2018, 348, 592-598.	12.7	87
197	Tailored synthesis of anatase–brookite heterojunction photocatalysts for degradation of cylindrospermopsin under UV–Vis light. Chemical Engineering Journal, 2017, 310, 428-436.	12.7	86
198	Unraveling different mechanisms of persulfate activation by graphite felt anode and cathode to destruct contaminants of emerging concern. Applied Catalysis B: Environmental, 2019, 253, 140-148.	20.2	86

#	Article	IF	CITATIONS
199	Single Fe atoms confined in two-dimensional MoS2 for sulfite activation: A biomimetic approach towards efficient radical generation. Applied Catalysis B: Environmental, 2020, 268, 118459.	20.2	86
200	Polymeric ultrafiltration membrane with in situ formed nano-silver within the inner pores for simultaneous separation and catalysis. Journal of Membrane Science, 2019, 579, 190-198.	8.2	85
201	Improving dewaterability and filterability of waste activated sludge by electrochemical Fenton pretreatment. Chemical Engineering Journal, 2019, 362, 525-536.	12.7	85
202	Degradation of microcystin-LR toxin by Fenton and Photo-Fenton processes. Toxicon, 2004, 43, 829-832.	1.6	84
203	One-step hydrothermal fabrication of visible-light-responsive AgInS2/SnIn4S8 heterojunction for highly-efficient photocatalytic treatment of organic pollutants and real pharmaceutical industry wastewater. Applied Catalysis B: Environmental, 2017, 219, 163-172.	20.2	84
204	Combined CdS nanoparticles-assisted photocatalysis and periphytic biological processes for nitrate removal. Chemical Engineering Journal, 2018, 353, 237-245.	12.7	84
205	Electrophilicity index as a critical indicator for the biodegradation of the pharmaceuticals in aerobic activated sludge processes. Water Research, 2019, 160, 10-17.	11.3	84
206	Reducing aquatic micropollutants – Increasing the focus on input prevention and integrated emission management. Science of the Total Environment, 2019, 652, 836-850.	8.0	84
207	Applications of anodized TiO2 nanotube arrays on the removal of aqueous contaminants of emerging concern: A review. Water Research, 2020, 186, 116327.	11.3	84
208	Bimodal mesoporous TiO2–P25 composite thick films with high photocatalytic activity and improved structural integrity. Applied Catalysis B: Environmental, 2008, 80, 147-155.	20.2	83
209	Mechanistic Study on the Role of Soluble Microbial Products in Sulfate Radical-Mediated Degradation of Pharmaceuticals. Environmental Science & amp; Technology, 2019, 53, 342-353.	10.0	83
210	Overlooked Formation of H ₂ O ₂ during the Hydroxyl Radical-Scavenging Process When Using Alcohols as Scavengers. Environmental Science & Technology, 2022, 56, 3386-3396.	10.0	83
211	Chapter 8 TiO2-Based Advanced Oxidation Nanotechnologies for Water Purification and Reuse. Sustainability Science and Engineering, 2010, 2, 229-254.	0.6	82
212	Electrochemical activation of persulfate on BDD and DSA anodes: Electrolyte influence, kinetics and mechanisms in the degradation of bisphenol A. Journal of Hazardous Materials, 2020, 388, 121789.	12.4	82
213	A comparative study on the removal of cylindrospermopsin and microcystins from water with NF-TiO2-P25 composite films with visible and UV–vis light photocatalytic activity. Applied Catalysis B: Environmental, 2012, 121-122, 30-39.	20.2	81
214	Chemical oxidation and reduction of hexachlorocyclohexanes: A review. Water Research, 2019, 162, 302-319.	11.3	81
215	Development of ozonation and reactive electrochemical membrane coupled process: Enhanced tetracycline mineralization and toxicity reduction. Chemical Engineering Journal, 2020, 383, 123149.	12.7	81
216	Abundance and distribution characteristics of microplastic in plateau cultivated land of Yunnan Province, China. Environmental Science and Pollution Research, 2021, 28, 1675-1688.	5.3	81

#	Article	IF	CITATIONS
217	Sorption and biodegradation of pharmaceuticals in aerobic activated sludge system: A combined experimental and theoretical mechanistic study. Chemical Engineering Journal, 2018, 342, 211-219.	12.7	80
218	Anion-Doped TiO ₂ Nanocatalysts for Water Purification under Visible Light. Industrial & Engineering Chemistry Research, 2013, 52, 13957-13964.	3.7	79
219	Prussian blue/TiO ₂ nanocomposites as a heterogeneous photo-Fenton catalyst for degradation of organic pollutants in water. Catalysis Science and Technology, 2015, 5, 504-514.	4.1	79
220	Treatment of winery wastewater by sulphate radicals: HSO 5 â~ /transition metal/UV-A LEDs. Chemical Engineering Journal, 2017, 310, 473-483.	12.7	79
221	An experimental and theoretical study on the degradation of clonidine by hydroxyl and sulfate radicals. Science of the Total Environment, 2020, 710, 136333.	8.0	79
222	Microwave-induced carbon nanotubes catalytic degradation of organic pollutants in aqueous solution. Journal of Hazardous Materials, 2016, 310, 226-234.	12.4	78
223	Nano-cerium oxide functionalized biochar for phosphate retention: preparation, optimization and rice paddy application. Chemosphere, 2017, 185, 816-825.	8.2	78
224	Degradation Mechanism of Cyanobacterial Toxin Cylindrospermopsin by Hydroxyl Radicals in Homogeneous UV/H ₂ O ₂ Process. Environmental Science & Technology, 2014, 48, 4495-4504.	10.0	77
225	Efficient degradation of lindane in aqueous solution by iron (II) and/or UV activated peroxymonosulfate. Journal of Photochemistry and Photobiology A: Chemistry, 2016, 316, 37-43.	3.9	77
226	Glucose and melamine derived nitrogen-doped carbonaceous catalyst for nonradical peroxymonosulfate activation. Carbon, 2020, 156, 399-409.	10.3	76
227	A critical review on the applications and potential risks of emerging MoS2 nanomaterials. Journal of Hazardous Materials, 2020, 399, 123057.	12.4	76
228	Recent Achievements in Development of TiO2-Based Composite Photocatalytic Materials for Solar Driven Water Purification and Water Splitting. Materials, 2020, 13, 1338.	2.9	76
229	Can We Effectively Degrade Microcystins? - Implications on Human Health. Anti-Cancer Agents in Medicinal Chemistry, 2011, 11, 19-37.	1.7	76
230	Impact of metal ions, metal oxides, and nanoparticles on the formation of disinfection byproducts during chlorination. Chemical Engineering Journal, 2017, 317, 777-792.	12.7	75
231	Mechanism of PCE oxidation by percarbonate in a chelated Fe(II)-based catalyzed system. Chemical Engineering Journal, 2015, 275, 53-62.	12.7	74
232	Susceptibility of the Algal Toxin Microcystin-LR to UV/Chlorine Process: Comparison with Chlorination. Environmental Science & amp; Technology, 2018, 52, 8252-8262.	10.0	74
233	Fabrication of novel Z-scheme SrTiO3/MnFe2O4 system with double-response activity for simultaneous microwave-induced and photocatalytic degradation of tetracycline and mechanism insight. Chemical Engineering Journal, 2020, 400, 125981.	12.7	74
234	NF-TiO2 photocatalysis of amitrole and atrazine with addition of oxidants under simulated solar light: Emerging synergies, degradation intermediates, and reusable attributes. Journal of Hazardous Materials, 2013, 260, 569-575.	12.4	73

#	Article	IF	CITATIONS
235	A visible-light-driven core-shell like Ag2S@Ag2CO3 composite photocatalyst with high performance in pollutants degradation. Chemosphere, 2016, 157, 250-261.	8.2	73
236	Innovative W-doped titanium dioxide anchored on clay for photocatalytic removal of atrazine. Catalysis Today, 2017, 280, 21-28.	4.4	73
237	Experimental and theoretical insight into hydroxyl and sulfate radicals-mediated degradation of carbamazepine. Environmental Pollution, 2020, 257, 113498.	7.5	73
238	Degradation and mineralization of organic UV absorber compound 2-phenylbenzimidazole-5-sulfonic acid (PBSA) using UV-254nm/H2O2. Journal of Hazardous Materials, 2015, 282, 233-240.	12.4	71
239	One-step in situ hydrothermal fabrication of octahedral CdS/SnIn4S8 nano-heterojunction for highly efficient photocatalytic treatment of nitrophenol and real pharmaceutical wastewater. Journal of Hazardous Materials, 2017, 340, 85-95.	12.4	71
240	Kinetics and Mechanism of Oxidation of Tryptophan by Ferrate(VI). Environmental Science & Technology, 2013, 47, 4572-4580.	10.0	70
241	Peroxymonosulfate catalytic degradation of persistent organic pollutants by engineered catalyst of self-doped iron/carbon nanocomposite derived from waste toner powder. Separation and Purification Technology, 2022, 291, 120963.	7.9	70
242	CLEAN WATER: water detoxification using innovative photocatalysts. Reviews in Environmental Science and Biotechnology, 2010, 9, 87-94.	8.1	69
243	Revealing the degradation intermediates and pathways of visible light-induced NF-TiO2 photocatalysis of microcystin-LR. Applied Catalysis B: Environmental, 2014, 154-155, 259-266.	20.2	69
244	A Mechanistic Understanding of Hydrogen Peroxide Decomposition by Vanadium Minerals for Diethyl Phthalate Degradation. Environmental Science & Technology, 2018, 52, 2178-2185.	10.0	69
245	Sources, transport, measurement and impact of nano and microplastics in urban watersheds. Reviews in Environmental Science and Biotechnology, 2020, 19, 275-336.	8.1	69
246	Catalytic combustion of toluene with La0.8Ce0.2MnO3 supported on CeO2 with different morphologies. Chemical Engineering Journal, 2016, 300, 300-305.	12.7	68
247	Efficient peroxymonosulfate activation and bisphenol A degradation derived from mineral-carbon materials: Key role of double mineral-templates. Applied Catalysis B: Environmental, 2020, 267, 118701.	20.2	68
248	Evaluating the Mechanism of Visible Light Activity for N,F-TiO ₂ Using Photoelectrochemistry. Journal of Physical Chemistry C, 2014, 118, 12206-12215.	3.1	67
249	Highly stable and covalently functionalized magnetic nanoparticles by polyethyleneimine for Cr(<scp>vi</scp>) adsorption in aqueous solution. RSC Advances, 2015, 5, 1398-1405.	3.6	67
250	Carbon-based TiO2 materials for the degradation of Microcystin-LA. Applied Catalysis B: Environmental, 2015, 170-171, 74-82.	20.2	66
251	Quantitative structure–activity relationship for the apparent rate constants of aromatic contaminants oxidized by ferrate (VI). Chemical Engineering Journal, 2017, 317, 258-266.	12.7	66
252	Modeling and optimization of heterogeneous Fenton-like and photo-Fenton processes using reusable Fe3O4-MWCNTs. Chemical Engineering Research and Design, 2019, 128, 273-283.	5.6	66

#	Article	IF	CITATIONS
253	Photoelectrochemical reactors for treatment of water and wastewater: a review. Environmental Chemistry Letters, 2020, 18, 1301-1318.	16.2	66
254	Degradation of contaminants of emerging concern by UV/H2O2 for water reuse: Kinetics, mechanisms, and cytotoxicity analysis. Water Research, 2020, 174, 115587.	11.3	66
255	Application of immobilized titanium dioxide photocatalysts for the degradation of creatinine and phenol, model organic contaminants found in NASA's spacecrafts wastewater streams. Catalysis Today, 2007, 124, 215-223.	4.4	65
256	<i>In situ</i> remediation of subsurface contamination: opportunities and challenges for nanotechnology and advanced materials. Environmental Science: Nano, 2019, 6, 1283-1302.	4.3	65
257	Cleaning chromium pollution in aquatic environments by bioremediation, photocatalytic remediation, electrochemical remediation and coupled remediation systems. Environmental Chemistry Letters, 2020, 18, 561-576.	16.2	65
258	Determination and Environmental Implications of Aqueous-Phase Rate Constants in Radical Reactions. Water Research, 2021, 190, 116746.	11.3	65
259	Biochar as a novel carbon-negative electron source and mediator: electron exchange capacity (EEC) and environmentally persistent free radicals (EPFRs): a review. Chemical Engineering Journal, 2022, 429, 132313.	12.7	65
260	Enhanced visible light photocatalytic activity of CN-codoped TiO2 films for the degradation of microcystin-LR. Journal of Molecular Catalysis A, 2013, 372, 58-65.	4.8	64
261	The fabrication of innovative single crystal N,F-codoped titanium dioxide nanowires with enhanced photocatalytic activity for degradation of atrazine. Applied Catalysis B: Environmental, 2015, 168-169, 550-558.	20.2	64
262	An innovative zinc oxide-coated zeolite adsorbent for removal of humic acid. Journal of Hazardous Materials, 2016, 313, 283-290.	12.4	64
263	Elimination of antibiotic resistance genes and control of horizontal transfer risk by UV-based treatment of drinking water: A mini review. Frontiers of Environmental Science and Engineering, 2019, 13, 1.	6.0	64
264	Effect of Oxygen in a Thin-Film Rotating Disk Photocatalytic Reactor. Environmental Science & Technology, 2002, 36, 3834-3843.	10.0	63
265	Elucidating sulfate radical-mediated disinfection profiles and mechanisms of Escherichia coli and Enterococcus faecalis in municipal wastewater. Water Research, 2020, 173, 115552.	11.3	63
266	Reactive High-Valent Iron Intermediates in Enhancing Treatment of Water by Ferrate. Environmental Science & Technology, 2022, 56, 30-47.	10.0	63
267	A 3D graphene-based biosensor as an early microcystin-LR screening tool in sources of drinking water supply. Electrochimica Acta, 2017, 236, 319-327.	5.2	62
268	The effect of solvent in the sol–gel synthesis of visible light-activated, sulfur-doped TiO2 nanostructured porous films for water treatment. Catalysis Today, 2014, 224, 132-139.	4.4	60
269	Decomposition of Iodinated Pharmaceuticals by UV-254 nm-assisted Advanced Oxidation Processes. Journal of Hazardous Materials, 2017, 323, 489-499.	12.4	60
270	Microwave hydrothermal-assisted preparation of novel spinel-NiFe 2 O 4 /natural mineral composites as microwave catalysts for degradation of aquatic organic pollutants. Journal of Hazardous Materials, 2018, 350, 1-9.	12.4	60

#	Article	IF	CITATIONS
271	Acetic acid functionalized TiO2/kaolinite composite photocatalysts with enhanced photocatalytic performance through regulating interfacial charge transfer. Journal of Catalysis, 2018, 367, 126-138.	6.2	60
272	Bismuth impregnated biochar for efficient estrone degradation: The synergistic effect between biochar and Bi/Bi2O3 for a high photocatalytic performance. Journal of Hazardous Materials, 2020, 384, 121258.	12.4	60
273	Homogeneous deposition-assisted synthesis of iron–nitrogen composites on graphene as highly efficient non-precious metal electrocatalysts for microbial fuel cell power generation. Journal of Power Sources, 2015, 278, 773-781.	7.8	59
274	Do membrane filtration systems in drinking water treatment plants release nano/microplastics?. Science of the Total Environment, 2021, 755, 142658.	8.0	59
275	Photogeneration of Reactive Species from Biochar-Derived Dissolved Black Carbon for the Degradation of Amine and Phenolic Pollutants. Environmental Science & Technology, 2021, 55, 8866-8876.	10.0	59
276	Internal electric field driving separation and migration of charge carriers via Z-scheme path in AgIn5S8/ZnO heterojunction for efficient decontamination of pharmaceutical pollutants. Chemical Engineering Journal, 2022, 428, 132096.	12.7	59
277	Hydroxyl radical generation by cactus-like copper oxide nanoporous carbon catalysts for microcystin-LR environmental remediation. Catalysis Science and Technology, 2016, 6, 530-544.	4.1	58
278	Kinetics and mechanisms of electrocatalytic hydrodechlorination of diclofenac on Pd-Ni/PPy-rGO/Ni electrodes. Applied Catalysis B: Environmental, 2020, 268, 118696.	20.2	58
279	Visible Light-Induced Catalyst-Free Activation of Peroxydisulfate: Pollutant-Dependent Production of Reactive Species. Environmental Science & amp; Technology, 2022, 56, 2626-2636.	10.0	58
280	Efficient degradation of clofibric acid by heterogeneous catalytic ozonation using CoFe2O4 catalyst in water. Journal of Hazardous Materials, 2021, 410, 124604.	12.4	57
281	A review of clay based photocatalysts: Role of phyllosilicate mineral in interfacial assembly, microstructure control and performance regulation. Chemosphere, 2021, 273, 129723.	8.2	57
282	Protection Mechanisms of Periphytic Biofilm to Photocatalytic Nanoparticle Exposure. Environmental Science & Technology, 2019, 53, 1585-1594.	10.0	56
283	Simultaneous regeneration of p-nitrophenol-saturated activated carbon fiber and mineralization of desorbed pollutants by electro-peroxone process. Carbon, 2016, 101, 399-408.	10.3	55
284	Distribution of organic phosphorus species in sediment profiles of shallow lakes and its effect on photo-release of phosphate during sediment resuspension. Environment International, 2019, 130, 104916.	10.0	55
285	Kinetics and mechanisms of the formation of chlorinated and oxygenated polycyclic aromatic hydrocarbons during chlorination. Chemical Engineering Journal, 2018, 351, 248-257.	12.7	54
286	Solar light induced photocatalytic activation of peroxymonosulfate by ultra-thin Ti3+ self-doped Fe2O3/TiO2 nanoflakes for the degradation of naphthalene. Applied Catalysis B: Environmental, 2022, 315, 121532.	20.2	54
287	TiO2 photocatalytic degradation and detoxification of cylindrospermopsin. Journal of Photochemistry and Photobiology A: Chemistry, 2015, 307-308, 115-122.	3.9	53
288	Effects of bromide on the degradation of organic contaminants with UV and Fe2+ activated persulfate. Chemical Engineering Journal, 2017, 318, 206-213.	12.7	53

#	Article	IF	CITATIONS
289	The effects of metallic engineered nanoparticles upon plant systems: An analytic examination of scientific evidence. Science of the Total Environment, 2017, 579, 93-106.	8.0	53
290	Adsorptive interaction of peroxymonosulfate with graphene and catalytic assessment via non-radical pathway for the removal of aqueous pharmaceuticals. Journal of Hazardous Materials, 2020, 384, 121340.	12.4	53
291	Degradation of highly chlorinated pesticide, lindane, in water using UV/persulfate: kinetics and mechanism, toxicity evaluation, and synergism by H2O2. Journal of Hazardous Materials, 2021, 402, 123558.	12.4	53
292	Origin of the improved reactivity of MoS2 single crystal by confining lattice Fe atom in peroxymonosulfate-based Fenton-like reaction. Applied Catalysis B: Environmental, 2021, 298, 120537.	20.2	53
293	Mineral Modulated Single Atom Catalyst for Effective Water Treatment. Advanced Functional Materials, 2022, 32, .	14.9	53
294	Nonmonotonic responses to low doses of xenoestrogens: A review. Environmental Research, 2017, 155, 199-207.	7.5	52
295	Environmental application of millimetre-scale sponge iron (s-Fe 0) particles (IV): New insights into visible light photo-Fenton-like process with optimum dosage of H 2 O 2 and RhB photosensitizers. Journal of Hazardous Materials, 2017, 323, 611-620.	12.4	52
296	Understanding synergistic mechanisms of ferrous iron activated sulfite oxidation and organic polymer flocculation for enhancing wastewater sludge dewaterability. Water Research, 2021, 189, 116652.	11.3	52
297	Microplastics separation and subsequent carbonization: Synthesis, characterization, and catalytic performance of iron/carbon nanocomposite. Journal of Cleaner Production, 2022, 330, 129901.	9.3	52
298	Synthesis of anatase nanostructured TiO2 particles at low temperature using ionic liquid for photocatalysis. Catalysis Communications, 2005, 6, 259-262.	3.3	51
299	Microcystin-LR removal from aqueous solutions using a magnetically separable N-doped TiO2 nanocomposite under visible light irradiation. Chemical Communications, 2013, 49, 10118.	4.1	51
300	Removal of strontium from drinking water by conventional treatment and lime softening in bench-scale studies. Water Research, 2016, 103, 319-333.	11.3	51
301	A ClO -mediated photoelectrochemical filtration system for highly-efficient and complete ammonia conversion. Journal of Hazardous Materials, 2020, 400, 123246.	12.4	51
302	Ag-decorated 3D flower-like Bi2MoO6/rGO with boosted photocatalytic performance for removal of organic pollutants. Rare Metals, 2021, 40, 1086-1098.	7.1	51
303	Non-negligible risk of chloropicrin formation during chlorination with the UV/persulfate pretreatment process in the presence of low concentrations of nitrite. Water Research, 2020, 168, 115194.	11.3	50
304	Mechanistic insight into superoxide radical-mediated degradation of carbon tetrachloride in aqueous solution: An in situ spectroscopic and computational study. Chemical Engineering Journal, 2021, 410, 128181.	12.7	49
305	Applications of computational chemistry, artificial intelligence, and machine learning in aquatic chemistry research. Chemical Engineering Journal, 2021, 426, 131810.	12.7	49
306	Comparative studies of various iron-mediated oxidative systems for the photochemical degradation of endosulfan in aqueous solution. Journal of Photochemistry and Photobiology A: Chemistry, 2015, 306, 80-86.	3.9	48

#	Article	IF	CITATIONS
307	Coadsorption and subsequent redox conversion behaviors of As(III) and Cr(VI) on Al-containing ferrihydrite. Environmental Pollution, 2018, 235, 660-669.	7.5	48
308	Ecotoxicological effects and removal of 17β-estradiol in chlorella algae. Ecotoxicology and Environmental Safety, 2019, 174, 377-383.	6.0	48
309	Surface-bound radical control rapid organic contaminant degradation through peroxymonosulfate activation by reduced Fe-bearing smectite clays. Journal of Hazardous Materials, 2020, 389, 121819.	12.4	48
310	Development of surfactant based electrochemical sensor for the trace level detection of mercury. Electrochimica Acta, 2016, 190, 1007-1014.	5.2	47
311	Electrochemically modified dissolved organic matter accelerates the combining photodegradation and biodegradation of 17α-ethinylestradiol in natural aquatic environment. Water Research, 2018, 137, 251-261.	11.3	47
312	Simultaneous regeneration of cathodic activated carbon fiber and mineralization of desorbed contaminations by electro-peroxydisulfate process: Advantages and limitations. Water Research, 2020, 171, 115456.	11.3	47
313	Development of photocatalysts for selective and efficient organic transformations. Journal of Photochemistry and Photobiology B: Biology, 2015, 148, 209-222.	3.8	45
314	Preparation of N,F-codoped TiO 2 nanoparticles by three different methods and comparison of visible-light photocatalytic performances. Separation and Purification Technology, 2017, 175, 305-313.	7.9	45
315	Construction of novel Z-scheme Ag/ZnFe2O4/Ag/BiTa1-xVxO4 system with enhanced electron transfer capacity for visible light photocatalytic degradation of sulfanilamide. Journal of Hazardous Materials, 2019, 375, 161-173.	12.4	45
316	Utilization of formic acid in nanoscale zero valent iron-catalyzed Fenton system for carbon tetrachloride degradation. Chemical Engineering Journal, 2020, 380, 122537.	12.7	45
317	Mechanistic Understanding of Superoxide Radical-Mediated Degradation of Perfluorocarboxylic Acids. Environmental Science & Technology, 2022, 56, 624-633.	10.0	45
318	Photodegradation of 17α-ethynylestradiol in dissolved humic substances solution: Kinetics, mechanism and estrogenicity variation. Journal of Environmental Sciences, 2017, 54, 196-205.	6.1	44
319	Efficient activation of peroxymonosulfate by copper sulfide for diethyl phthalate degradation: Performance, radical generation and mechanism. Science of the Total Environment, 2020, 749, 142387.	8.0	44
320	Manganese doped iron–carbon composite for synergistic persulfate activation: Reactivity, stability, and mechanism. Journal of Hazardous Materials, 2021, 405, 124228.	12.4	44
321	Ecotoxicological Assessment of Microplastics in Freshwater Sources—A Review. Water (Switzerland), 2021, 13, 56.	2.7	44
322	Monitoring of 2-butanone using a Ag–Cu bimetallic alloy nanoscale electrochemical sensor. RSC Advances, 2015, 5, 44427-44434.	3.6	43
323	Mitigating 17α-ethynylestradiol water contamination through binding and photosensitization by dissolved humic substances. Journal of Hazardous Materials, 2017, 327, 197-205.	12.4	43
324	Holistic sludge management through ozonation: A critical review. Journal of Environmental Management, 2017, 185, 79-95.	7.8	43

#	Article	IF	CITATIONS
325	A novel HCV electrochemical biosensor based on a polyaniline@Ni-MOF nanocomposite. Dalton Transactions, 2020, 49, 8918-8926.	3.3	43
326	Bi2WO6-TiO2/starch composite films with Ag nanoparticle irradiated by γ-ray used for the visible light photocatalytic degradation of ethylene. Chemical Engineering Journal, 2021, 421, 129986.	12.7	43
327	UV365 induced elimination of contaminants of emerging concern in the presence of residual nitrite: Roles of reactive nitrogen species. Water Research, 2020, 178, 115829.	11.3	42
328	Influencing factors and health risk assessment of polycyclic aromatic hydrocarbons in groundwater in China. Journal of Hazardous Materials, 2021, 402, 123419.	12.4	42
329	Effects and bioaccumulation of 17β-estradiol and 17α-ethynylestradiol following long-term exposure in crucian carp. Ecotoxicology and Environmental Safety, 2015, 112, 169-176.	6.0	41
330	Simultaneous disinfection of E.Âfaecalis and degradation of carbamazepine by sulfate radicals: An experimental and modelling study. Environmental Pollution, 2020, 263, 114558.	7.5	41
331	Identification of TiO2 photocatalytic destruction byproducts and reaction pathway of cylindrospermopsin. Applied Catalysis B: Environmental, 2015, 163, 591-598.	20.2	40
332	Fabrication of Hierarchically Porous Reduced Graphene Oxide/SnIn4S8 Composites by a Low-Temperature Co-Precipitation Strategy and Their Excellent Visible-Light Photocatalytic Mineralization Performance. Catalysts, 2016, 6, 113.	3.5	40
333	Fe-Chelated polymer templated graphene aerogel with enhanced Fenton-like efficiency for water treatment. Environmental Science: Nano, 2019, 6, 3232-3241.	4.3	40
334	Nitrogen conversion from ammonia to trichloronitromethane: Potential risk during UV/chlorine process. Water Research, 2020, 172, 115508.	11.3	40
335	Self-Powered Water Flow-Triggered Piezocatalytic Generation of Reactive Oxygen Species for Water Purification in Simulated Water Drainage. ACS ES&T Engineering, 2022, 2, 101-109.	7.6	40
336	A comprehensive review on algae removal and control by coagulation-based processes: mechanism, material, and application. Separation and Purification Technology, 2022, 293, 121106.	7.9	40
337	Nanodiamond–TiO ₂ composites for photocatalytic degradation of microcystin-LA in aqueous solutions under simulated solar light. RSC Advances, 2015, 5, 58363-58370.	3.6	39
338	Assessment of nitrogen–fluorine-codoped TiO2 under visible light for degradation of BPA: Implication for field remediation. Journal of Photochemistry and Photobiology A: Chemistry, 2016, 314, 81-92.	3.9	39
339	Adsorption of heavy metal from aqueous solution by dehydrated root powder of long-root <i>Eichhornia crassipes</i> . International Journal of Phytoremediation, 2016, 18, 103-109.	3.1	39
340	Solar photo-Fenton treatment of microcystin-LR in aqueous environment: Transformation products and toxicity in different water matrices. Journal of Hazardous Materials, 2018, 349, 282-292.	12.4	39
341	Ultraviolet–Visible Light–Sensitive High Surface Area Phosphorous-Fluorine–Co-Doped TiO ₂ Nanoparticles for the Degradation of Atrazine in Water. Environmental Engineering Science, 2014, 31, 435-446.	1.6	38
342	Removal of diclofenac from water by zeolite-assisted advanced oxidation processes. Journal of Photochemistry and Photobiology A: Chemistry, 2016, 321, 238-247.	3.9	38

#	Article	IF	CITATIONS
343	Electrochemical treatment of bio-treated landfill leachate: Influence of electrode arrangement, potential, and characteristics. Chemical Engineering Journal, 2018, 344, 34-41.	12.7	38
344	A New Concept of Promoting Nitrate Reduction in Surface Waters: Simultaneous Supplement of Denitrifiers, Electron Donor Pool, and Electron Mediators. Environmental Science & Technology, 2018, 52, 8617-8626.	10.0	38
345	Novel biosorbents synthesized from fungal and bacterial biomass and their applications in the adsorption of volatile organic compounds. Bioresource Technology, 2020, 300, 122705.	9.6	38
346	CTAB–intercalated molybdenum disulfide nanosheets for enhanced simultaneous removal of Cr(VI) and Ni(II) from aqueous solutions. Journal of Hazardous Materials, 2020, 396, 122728.	12.4	38
347	Ultraviolet light-mediated activation of persulfate for the degradation of cobalt cyanocomplexes. Journal of Hazardous Materials, 2020, 392, 122389.	12.4	38
348	TiO2-carbon microspheres as photocatalysts for effective remediation of pharmaceuticals under simulated solar light. Separation and Purification Technology, 2021, 275, 119169.	7.9	38
349	Effect of surfactant in a modified sol on the physicochemical properties and photocatalytic activity of crystalline TiO2 nanoparticles. Topics in Catalysis, 2007, 44, 513-521.	2.8	37
350	Phosphate removal using modified Bayoxide® E33 adsorption media. Environmental Science: Water Research and Technology, 2015, 1, 96-107.	2.4	37
351	Comparative toxicity reduction potential of UV/sodium percarbonate and UV/hydrogen peroxide treatments for bisphenol A in water: An integrated analysis using chemical, computational, biological, and metabolomic approaches. Water Research, 2021, 190, 116755.	11.3	37
352	Novel franklinite-like synthetic zinc-ferrite redox nanomaterial: synthesis, and evaluation for degradation of diclofenac in water. Applied Catalysis B: Environmental, 2020, 275, 119098.	20.2	37
353	Confirmation of hydroxyl radicals (•OH) generated in the presence of TiO2 supported on AC under microwave irradiation. Journal of Hazardous Materials, 2014, 278, 152-157.	12.4	36
354	Peroxymonosulfate/solar radiation process for the removal of aqueous microcontaminants. Kinetic modeling, influence of variables and matrix constituents. Journal of Hazardous Materials, 2020, 400, 123118.	12.4	36
355	In Situ Technologies for Reclamation of PCB-Contaminated Sediments: Current Challenges and Research Thrust Areas. Journal of Environmental Engineering, ASCE, 2007, 133, 1075-1078.	1.4	35
356	Electro-peroxone regeneration of phenol-saturated activated carbon fiber: The effects of irreversible adsorption and operational parameters. Carbon, 2016, 109, 321-330.	10.3	35
357	Impact of leaching conditions on constituents release from Flue Gas Desulfurization Gypsum (FGDG) and FGDG-soil mixture. Journal of Hazardous Materials, 2017, 324, 83-93.	12.4	35
358	New Insight into a Fenton-like Reaction Mechanism over Sulfidated β-FeOOH: Key Role of Sulfidation in Efficient Iron(III) Reduction and Sulfate Radical Generation. Environmental Science & Technology, 2022, 56, 5542-5551.	10.0	35
359	Synthesis, characterization and electrochemical properties of mesoporous zirconia nanomaterials prepared by self-assembling sol–gel method with Tween 20 as a template. Chemical Engineering Journal, 2011, 170, 518-524.	12.7	34
360	Solar-driven photocatalytic treatment of diclofenac using immobilized TiO2-based zeolite composites. Environmental Science and Pollution Research, 2016, 23, 17982-17994.	5.3	34

#	Article	IF	CITATIONS
361	Efficient degradation of lindane by visible and simulated solar light-assisted S-TiO2/peroxymonosulfate process: Kinetics and mechanistic investigations. Molecular Catalysis, 2017, 428, 9-16.	2.0	34
362	Combinatorial anti-proliferative effects of tamoxifen and naringenin: The role of four estrogen receptor subtypes. Toxicology, 2018, 410, 231-246.	4.2	34
363	Modified humic acids mediate efficient mineralization in a photo-bio-electro-Fenton process. Water Research, 2021, 190, 116740.	11.3	34
364	Activation of inorganic peroxides with magnetic graphene for the removal of antibiotics from wastewater. Environmental Science: Nano, 2021, 8, 960-977.	4.3	34
365	Solvothermal synthesis of P25/Bi2WO6 nanocomposite photocatalyst and photocatalytic degradation of ethylene under visible light. Applied Surface Science, 2018, 439, 815-822.	6.1	33
366	Cotransformation of Carbon Dots and Contaminant under Light in Aqueous Solutions: A Mechanistic Study. Environmental Science & Technology, 2019, 53, 6235-6244.	10.0	33
367	An N,S-Anchored Single-Atom Catalyst Derived from Domestic Waste for Environmental Remediation. ACS ES&T Engineering, 2021, 1, 1460-1469.	7.6	33
368	Photochemical characterization of paddy water during rice cultivation: Formation of reactive intermediates for As(III) oxidation. Water Research, 2021, 206, 117721.	11.3	33
369	Photocatalytic activity and electrochemical response of titania film with macro/mesoporous texture. Thin Solid Films, 2008, 516, 7930-7936.	1.8	32
370	Degradation of cylindrospermopsin by using polymorphic titanium dioxide under UV–Vis irradiation. Catalysis Today, 2014, 224, 49-55.	4.4	32
371	Dissolved organic matter as a terminal electron acceptor in the microbial oxidation of steroid estrogen. Environmental Pollution, 2016, 218, 26-33.	7.5	32
372	Electrochemical Enhancement of Photocatalytic Disinfection on Aligned TiO2 and Nitrogen Doped TiO2 Nanotubes. Molecules, 2017, 22, 704.	3.8	32
373	Hydrogel as a miniature hydrogen production reactor to enhance photocatalytic hydrogen evolution activities of CdS and ZnS quantum dots derived from modified gel crystal growth method. Chemical Engineering Journal, 2019, 373, 814-820.	12.7	32
374	Selective Reduction of Cr(VI) in Chromium, Copper and Arsenic (CCA) Mixed Waste Streams Using UV/TiO2 Photocatalysis. Molecules, 2015, 20, 2622-2635.	3.8	31
375	Industrial synthesis and characterization of nanophotocatalysts materials: titania. Nanotechnology Reviews, 2016, 5, 467-479.	5.8	31
376	Revealing the mechanism, pathways and kinetics of UV254nm/H2O2-based degradation of model active sunscreen ingredient PBSA. Chemical Engineering Journal, 2016, 288, 824-833.	12.7	31
377	Unique surface structure of nano-sized CulnS2 anchored on rGO thin film and its superior photocatalytic activity in real wastewater treatment. Chemical Engineering Journal, 2018, 338, 591-598.	12.7	31
378	Detoxification of municipal solid waste incinerator (MSWI) fly ash by single-mode microwave (MW) irradiation: Addition of urea on the degradation of Dioxin and mechanism. Journal of Hazardous Materials, 2019, 369, 279-289.	12.4	31

#	Article	IF	CITATIONS
379	Environmentally friendly synthesized and magnetically recoverable designed ferrite photo-catalysts for wastewater treatment applications. Journal of Hazardous Materials, 2020, 381, 121200.	12.4	31
380	High-performance and stable Ru-Pd nanosphere catalyst supported on two-dimensional boron nitride nanosheets for the hydrogenation of furfural via water-mediated protonation. Fuel, 2021, 290, 119826.	6.4	31
381	Insight into the visible light activation of sulfite by Fe/g-C3N4 with rich N vacancies for pollutant removal and sterilization: A novel approach for enhanced generation of oxysulfur radical. Chemical Engineering Journal, 2022, 438, 135663.	12.7	31
382	Investigation of the photocatalytic degradation pathway of the urine metabolite, creatinine: The effect of pH. Water Research, 2009, 43, 3956-3963.	11.3	30
383	Photocatalytic oxidation of nitrogen oxides on N-F-doped titania thin films. Applied Catalysis B: Environmental, 2013, 140-141, 619-625.	20.2	30
384	Ozonation of Cylindrospermopsin (Cyanotoxin): Degradation Mechanisms and Cytotoxicity Assessments. Environmental Science & Technology, 2016, 50, 1437-1446.	10.0	30
385	Enhanced visible-light photoelectrochemical hydrogen evolution through degradation of methyl orange in a cell based on coral-like Pt-deposited TiO2 thin film with sub-2 nm pores. Catalysis Today, 2019, 335, 333-344.	4.4	30
386	lsotope ratio mass spectrometry and spectroscopic techniques for microplastics characterization. Talanta, 2021, 224, 121743.	5.5	30
387	Effects of pH and dissolved oxygen on the photodegradation of 17α-ethynylestradiol in dissolved humic acid solution. Environmental Sciences: Processes and Impacts, 2016, 18, 78-86.	3.5	29
388	Rational design of efficient visible-light driven photocatalyst through 0D/2D structural assembly: Natural kaolinite supported monodispersed TiO2 with carbon regulation. Chemical Engineering Journal, 2020, 396, 125311.	12.7	29
389	Differences of cell surface characteristics between the bacterium Pseudomonas veronii and fungus Ophiostoma stenoceras and their different adsorption properties to hydrophobic organic compounds. Science of the Total Environment, 2019, 650, 2095-2106.	8.0	28
390	Molecular identification guided process design for advanced treatment of electroless nickel plating effluent. Water Research, 2020, 168, 115211.	11.3	28
391	Solar light-assisted remediation of domestic wastewater by NB-TiO2 nanoparticles for potable reuse. Applied Catalysis B: Environmental, 2020, 269, 118807.	20.2	28
392	Novel microwave-driven synthesis of hydrophilic polyvinylidene fluoride/polyacrylic acid (PVDF/PAA) membranes and decoration with nano zero-valent-iron (nZVI) for water treatment applications. Journal of Membrane Science, 2021, 620, 118817.	8.2	28
393	One–step reductive synthesis of Ti3+ self–doped elongated anatase TiO2 nanowires combined with reduced graphene oxide for adsorbing and degrading waste engine oil. Journal of Hazardous Materials, 2019, 378, 120752.	12.4	27
394	Photoelectrocatalytic simultaneous removal of 17α-ethinylestradiol and E. coli using the anode of Ag and SnO2-Sb 3D-loaded TiO2 nanotube arrays. Journal of Hazardous Materials, 2020, 398, 122805.	12.4	27
395	Alternative synthesis of nitrogen and carbon co-doped TiO2 for removing fluoroquinolone antibiotics in water under visible light. Catalysis Today, 2021, 361, 11-16.	4.4	27
396	A streptavidin functionalized graphene oxide/Au nanoparticles composite for the construction of sensitive chemiluminescent immunosensor. Analytica Chimica Acta, 2014, 839, 67-73.	5.4	26

#	Article	IF	CITATIONS
397	Photocatalysis for disinfection and removal of contaminants of emerging concern. Chemical Engineering Journal, 2015, 261, 1-2.	12.7	26
398	Simultaneous photocatalytic degradation of ibuprofen and H2 evolution over Au/sheaf-like TiO2 mesocrystals. Chemosphere, 2020, 261, 127759.	8.2	26
399	Hydroxyl Radical-Involving <i>p</i> -Nitrophenol Oxidation during Its Reduction by Nanoscale Sulfidated Zerovalent Iron under Anaerobic Conditions. Environmental Science & Technology, 2021, 55, 2403-2410.	10.0	26
400	Tube-in-tube membrane photoreactor as a new technology to boost sulfate radical advanced oxidation processes. Water Research, 2021, 191, 116815.	11.3	26
401	Enhanced degradation of sulfamethoxazole by a modified nano zero-valent iron with a β-cyclodextrin polymer: Mechanism and toxicity evaluation. Science of the Total Environment, 2022, 817, 152888.	8.0	26
402	Environmental application of millimeter-scale sponge iron (s-FeO) particles (II): The effect of surface copper. Journal of Hazardous Materials, 2015, 287, 325-334.	12.4	25
403	Coupling electrochemical and biological methods for 17α-ethinylestradiol removal from water by different microorganisms. Journal of Hazardous Materials, 2017, 340, 120-129.	12.4	25
404	Near UVâ€Irradiation of CuO _x â€Impregnated TiO ₂ Providing Active Species for H ₂ Production Through Methanol Photoreforming. ChemCatChem, 2019, 11, 4314-4326.	3.7	25
405	Distribution characteristics and health risk assessment of volatile organic compounds in the groundwater of Lanzhou City, China. Environmental Geochemistry and Health, 2020, 42, 3609-3622.	3.4	25
406	Kinetics and mechanistic aspects of removal of heavy metal through gas-liquid sulfide precipitation: A computational and experimental study. Journal of Hazardous Materials, 2021, 408, 124868.	12.4	25
407	Transformation of phenol and nitrobenzene by superoxide radicals: Kinetics and mechanisms. Chemical Engineering Journal, 2022, 442, 136134.	12.7	25
408	Chapter Green Nanotechnology: Development of Nanomaterials for Environmental and Energy Applications. ACS Symposium Series, 2013, , 201-229.	0.5	24
409	The Functional Mechanisms and Application of Electron Shuttles in Extracellular Electron Transfer. Current Microbiology, 2018, 75, 99-106.	2.2	24
410	Dissolution of silver nanoparticles in colloidal consumer products: effects of particle size and capping agent. Journal of Nanoparticle Research, 2019, 21, 1-155.	1.9	24
411	A novel array of double dielectric barrier discharge combined with Ti Co catalyst to remove high-flow-rate toluene: Performance evaluation and mechanism analysis. Science of the Total Environment, 2019, 692, 940-951.	8.0	24
412	Key structural features promoting radical driven degradation of emerging contaminants in water. Environment International, 2019, 124, 38-48.	10.0	24
413	Exhaustive Photocatalytic Lindane Degradation by Combined Simulated Solar Light-Activated Nanocrystalline TiO2 and Inorganic Oxidants. Catalysts, 2019, 9, 425.	3.5	24
414	Dual-functional paired photoelectrocatalytic system for the photocathodic reduction of CO2 to fuels and the anodic oxidation of furfural to value-added chemicals. Applied Catalysis B: Environmental, 2021, 298, 120520.	20.2	24

#	Article	IF	CITATIONS
415	Desorption of Pentachlorophenol from Soils Using Mixed Solvents. Environmental Science & Technology, 1999, 33, 4483-4491.	10.0	23
416	An innovative nutritional slow-release packing material with functional microorganisms for biofiltration: Characterization and performance evaluation. Journal of Hazardous Materials, 2019, 366, 16-26.	12.4	23
417	Susceptibility of atrazine photo-degradation in the presence of nitrate: Impact of wavelengths and significant role of reactive nitrogen species. Journal of Hazardous Materials, 2020, 388, 121760.	12.4	23
418	Degradation of contaminants of emerging concern in UV/Sodium percarbonate Process: Kinetic understanding of carbonate radical and energy consumption evaluation. Chemical Engineering Journal, 2022, 442, 135995.	12.7	23
419	Remediation of Chemically-Contaminated Waters Using Sulfate Radical Reactions: Kinetic Studies. ACS Symposium Series, 2011, , 247-263.	0.5	22
420	Photobleaching alters the photochemical and biological reactivity of humic acid towards 17α-ethynylestradiol. Environmental Pollution, 2017, 220, 1386-1393.	7.5	22
421	Magnetically recoverable TiO2-WO3 photocatalyst to oxidize bisphenol A from model wastewater under simulated solar light. Environmental Science and Pollution Research, 2017, 24, 12589-12598.	5.3	22
422	The microbial transformation of 17l2‑estradiol in an anaerobic aqueous environment is mediated by changes in the biological properties of natural dissolved organic matter. Science of the Total Environment, 2018, 631-632, 641-648.	8.0	22
423	Fe(III)-oxalate complex mediated phosphate released from diazinon photodegradation: Pathway signatures based on oxygen isotopes. Journal of Hazardous Materials, 2018, 358, 319-326.	12.4	22
424	Facile synthesis of amino-functional large-size mesoporous silica sphere and its application for Pb2+ removal. Journal of Hazardous Materials, 2019, 378, 120664.	12.4	22
425	Assessment of solar-assisted electrooxidation of bisphenol AF and bisphenol A on boron-doped diamond electrodes. Environmental Science and Ecotechnology, 2020, 3, 100036.	13.5	22
426	Tailored BiVO4 for enhanced visible-light photocatalytic performance. Journal of Environmental Chemical Engineering, 2021, 9, 106025.	6.7	22
427	Extraction of Chlorophenols from Water Using Room Temperature Ionic Liquids. ACS Symposium Series, 2003, , 544-560.	0.5	21
428	Photodegradation of pentachlorophenol in room temperature ionic liquids. Journal of Photochemistry and Photobiology A: Chemistry, 2007, 192, 114-121.	3.9	21
429	Overview: Harmful algal blooms and natural toxins in fresh and marine waters – Exposure, occurrence, detection, toxicity, control, management and policy. Toxicon, 2010, 55, 907-908.	1.6	21
430	Combination of multi-oxidation process and electrolysis for pretreatment of PCB industry wastewater and recovery of highly-purified copper. Chemical Engineering Journal, 2018, 354, 228-236.	12.7	21
431	Optimization of Synthesis Conditions of Carbon Nanotubes via Ultrasonic-Assisted Floating Catalyst Deposition Using Response Surface Methodology. Nanomaterials, 2018, 8, 316.	4.1	21
432	Simulated solar photo-assisted decomposition of peroxymonosulfate. Radiation filtering and operational variables influence on the oxidation of aqueous bezafibrate. Water Research, 2019, 162, 383-393.	11.3	21

#	Article	IF	CITATIONS
433	New insight into the cosolvent effect on the degradation of tetrabromobisphenol A (TBBPA) over millimeter-scale palladised sponge iron (Pd-s-FeO) particles. Chemical Engineering Journal, 2019, 361, 1423-1436.	12.7	21
434	Formation and enhanced photodegradation of chlorinated derivatives of bisphenol A in wastewater treatment plant effluent. Water Research, 2020, 184, 116002.	11.3	21
435	Formation of Nitrite and Hydrogen Peroxide in Water during the Vacuum Ultraviolet Irradiation Process: Impacts of pH, Dissolved Oxygen, and Nitrate Concentration. Environmental Science & Technology, 2021, 55, 1682-1689.	10.0	21
436	Highly efficient photoelectrocatalytic degradation of cefotaxime sodium on the MoSe2/TiO2 nanotubes photoanode with abundant oxygen vacancies. Journal of Solid State Chemistry, 2021, 303, 122455.	2.9	21
437	Adsorption behavior and mechanism of ibuprofen onto BiOCl microspheres with exposed {001} facets. Environmental Science and Pollution Research, 2017, 24, 9556-9565.	5.3	20
438	Alterations of lead speciation by sulfate from addition of flue gas desulfurization gypsum (FGDG) in two contaminated soils. Science of the Total Environment, 2017, 575, 1522-1529.	8.0	20
439	Design and preparation of SnO2/SnS2/conjugated polyvinyl chloride derivative ternary composite with enhanced visible-light photocatalytic activity. Materials Research Bulletin, 2019, 118, 110524.	5.2	20
440	Electrochemical reductive remediation of trichloroethylene contaminated groundwater using biomimetic iron-nitrogen-doped carbon. Journal of Hazardous Materials, 2021, 419, 126458.	12.4	20
441	Solar light assisted photocatalytic degradation of 1,4-dioxane using high temperature stable anatase W-TiO2 nanocomposites. Catalysis Today, 2021, 380, 199-208.	4.4	20
442	Photoelectrocatalytic coupling system synergistically removal of antibiotics and antibiotic resistant bacteria from aquatic environment. Journal of Hazardous Materials, 2022, 424, 127553.	12.4	20
443	Degradation of mineral-immobilized pyrene by ferrate oxidation: Role of mineral type and intermediate oxidative iron species. Water Research, 2022, 217, 118377.	11.3	20
444	UV/Sodium percarbonate for bisphenol A treatment in water: Impact of water quality parameters on the formation of reactive radicals. Water Research, 2022, 219, 118457.	11.3	20
445	Photocatalytic cellulosic electrospun fibers for the degradation of potent cyanobacteria toxin microcystin-LR. Journal of Materials Chemistry, 2012, 22, 12666.	6.7	19
446	Environmental application of millimetre-scale sponge iron (s-FeO) particles (I): Pretreatment of cationic triphenylmethane dyes. Journal of Hazardous Materials, 2015, 283, 469-479.	12.4	19
447	Efficient degradation of cytotoxic contaminants of emerging concern by UV/H ₂ O ₂ . Environmental Science: Water Research and Technology, 2018, 4, 1272-1281.	2.4	19
448	Double-network hydrogel templated FeS/graphene with enhanced PMS activation performance: considering the effect of the template and iron species. Environmental Science: Nano, 2020, 7, 817-828.	4.3	19
449	Construction of TiO2@Bi2WO6 hollow microspheres by template method for enhanced degradation of ethylene under visible light. Optical Materials, 2021, 113, 110839.	3.6	19
450	Production of polyhydroxyalkanoates from propylene oxide saponification wastewater residual sludge using volatile fatty acids and bacterial community succession. Bioresource Technology, 2021, 329, 124912.	9.6	19

#	Article	IF	CITATIONS
451	Degradation of dibutyl phthalate (DBP) by UV-254Ânm/H2O2 photochemical oxidation: kinetics and influence of various process parameters. Environmental Science and Pollution Research, 2016, 23, 23772-23780.	5.3	18
452	Reuse of TiO 2 -based catalyst for solar driven water treatment; thermal and chemical reactivation. Journal of Photochemistry and Photobiology A: Chemistry, 2017, 333, 117-129.	3.9	18
453	The modulatory role of low concentrations of bisphenol A on tamoxifen-induced proliferation and apoptosis in breast cancer cells. Environmental Science and Pollution Research, 2019, 26, 2353-2362.	5.3	18
454	Enhancing the performance of Fenton-like oxidation by a dual-layer membrane: A sequential interception-oxidation process. Journal of Hazardous Materials, 2021, 402, 123766.	12.4	18
455	Double-dose responses of Scenedesmus capricornus microalgae exposed to humic acid. Science of the Total Environment, 2022, 806, 150547.	8.0	18
456	Elbaite catalyze peroxymonosulfate for advanced oxidation of organic pollutants: Hydroxyl groups induced generation of reactive oxygen species. Journal of Hazardous Materials, 2020, 398, 122932.	12.4	18
457	Photocatalytic activation of peroxydisulfate by a new porous g-C3N4/reduced graphene oxide/TiO2 nanobelts composite for efficient degradation of 17α-ethinylestradiol. Chemical Engineering Journal, 2022, 446, 137325.	12.7	18
458	Simple Procedure of Making Room Temperature Mesoporous TiO2 Films with High Purity and Enhanced Photocatalytic Activity. Environmental Engineering Science, 2007, 24, 13-20.	1.6	17
459	Could microwave induced catalytic oxidation (MICO) process over CoFe2O4 effectively eliminate brilliant green in aqueous solution?. Journal of Hazardous Materials, 2013, 263, 600-609.	12.4	17
460	Environmental application of millimetre-scale sponge iron (s-FeO) particles (III): The effect of surface silver. Journal of Hazardous Materials, 2015, 299, 618-629.	12.4	17
461	Enhanced biotic and abiotic transformation of Cr(<scp>vi</scp>) by quinone-reducing bacteria/dissolved organic matter/Fe(<scp>iii</scp>) in anaerobic environment. Environmental Sciences: Processes and Impacts, 2016, 18, 1185-1192.	3.5	17
462	Using H2O2 treatments for the degradation of cyanobacteria and microcystins in a shallow hypertrophic reservoir. Environmental Science and Pollution Research, 2016, 23, 21523-21535.	5.3	17
463	Research progress on the reproductive and non-reproductive endocrine tumors by estrogen-related receptors. Journal of Steroid Biochemistry and Molecular Biology, 2016, 158, 22-30.	2.5	17
464	Enhanced effect of EDDS and hydroxylamine on Fe(II)-catalyzed SPC system for trichloroethylene degradation. Environmental Science and Pollution Research, 2018, 25, 15733-15742.	5.3	17
465	Simulation study on comparison of algal treatment to conventional biological processes for greywater treatment. Algal Research, 2018, 35, 106-114.	4.6	17
466	Preparation of SnO2/conjugated polyvinyl alcohol derivative nanohybrid with good performance in visible light-induced photocatalytic reduction of Cr(VI). Materials Science in Semiconductor Processing, 2019, 102, 104586.	4.0	17
467	Photocatalytic degradation of dye by Ag/TiO2 nanoparticles prepared with different sol–gel crystallization in the presence of effluent organic matter. Environmental Science and Pollution Research, 2019, 26, 35900-35912.	5.3	17
468	Graphene-modified graphite paper cathode for the efficient bioelectrochemical removal of chromium. Chemical Engineering Journal, 2021, 405, 126545.	12.7	17

#	Article	IF	CITATIONS
469	Molybdenum disulfide nanosheets vertically grown on self-supported titanium dioxide/nitrogen-doped carbon nanofiber film for effective hydrogen peroxide decomposition and "memory catalysis― Journal of Colloid and Interface Science, 2021, 596, 384-395.	9.4	17
470	Sources and Occurrence of Cyanotoxins Worldwide. Environmental Pollution, 2010, , 101-127.	0.4	17
471	Reevaluation of the Reactivity of Superoxide Radicals with a Sulfonamide Antibiotic, Sulfacetamide: An Experimental and Theoretical Study. ACS ES&T Water, 2021, 1, 2339-2347.	4.6	17
472	Interplay of bicarbonate and the oxygen-containing groups of carbon nanotubes dominated the metal-free activation of peroxymonosulfate. Chemical Engineering Journal, 2022, 430, 133102.	12.7	17
473	Mechanistic Study of the Effects of Agricultural Amendments on Photochemical Processes in Paddy Water during Rice Growth. Environmental Science & Technology, 2022, 56, 4221-4230.	10.0	17
474	Fabrication of 2D sheet-like BiOCl/carbon quantum dot hybrids via a template-free coprecipitation method and their tunable visible-light photocatalytic activities derived from different size distributions of carbon quantum dots. Nanotechnology, 2016, 27, 065701.	2.6	16
475	Quantification of carbon nanotubes in different environmental matrices by a microwave induced heating method. Science of the Total Environment, 2017, 580, 509-517.	8.0	16
476	TiO2-SnS2 nanocomposites: solar-active photocatalytic materials for water treatment. Environmental Science and Pollution Research, 2017, 24, 19965-19979.	5.3	16
477	Removing Escherichia coli from water using zinc oxide-coated zeolite. Water Research, 2018, 141, 145-151.	11.3	16
478	The influence of a washing pretreatment containing phosphate anions on single-mode microwave-based detoxification of fly ash from municipal solid waste incinerators. Chemical Engineering Journal, 2020, 387, 124053.	12.7	16
479	Solvent-free synthesis of MFI-type zeolites and their degradation properties of gas-phase styrene. Journal of Hazardous Materials, 2020, 397, 122630.	12.4	16
480	Optimizing and understanding the pressurized vertical electro-osmotic dewatering of activated sludge. Chemical Engineering Research and Design, 2020, 140, 392-402.	5.6	16
481	Synthesis and enhanced photocatalytic performance of 0D/2D CuO/tourmaline composite photocatalysts. Beilstein Journal of Nanotechnology, 2020, 11, 407-416.	2.8	16
482	Effects of Experimental Conditions on the Signaling Fidelity of Impedance-Based Nucleic Acid Sensors. Analytical Chemistry, 2021, 93, 812-819.	6.5	16
483	Adsorption and photochemical capacity on 17α-ethinylestradiol by char produced in the thermo treatment process of plastic waste. Journal of Hazardous Materials, 2022, 423, 127066.	12.4	16
484	A comparative study of the degradation efficiency of chlorinated organic compounds by bimetallic zero-valent iron nanoparticles. Environmental Science: Water Research and Technology, 2021, 8, 162-172.	2.4	16
485	Making waves: Defining advanced reduction technologies from the perspective of water treatment. Water Research, 2022, 212, 118101.	11.3	16
486	Analysis of the Electrochemical Oxidation of Multiwalled Carbon Nanotube Tower Electrodes in Sodium Hydroxide. Electroanalysis, 2012, 24, 1501-1508.	2.9	15

#	Article	IF	CITATIONS
487	An enzymatic glucose biosensor based on a glassy carbon electrode modified with cylinder-shaped titanium dioxide nanorods. Mikrochimica Acta, 2015, 182, 1841-1848.	5.0	15
488	Zero-valent iron impregnated cellulose acetate mixed matrix membranes for the treatment of textile industry effluent. RSC Advances, 2015, 5, 62486-62497.	3.6	15
489	Stimulated dissolved organic matter by electrochemical route to produce activity substances for removing of 17 α -ethinylestradiol. Journal of Electroanalytical Chemistry, 2016, 780, 233-240.	3.8	15
490	Near real-time measurement of carbonaceous aerosol using microplasma spectroscopy: Application to measurement of carbon nanomaterials. Aerosol Science and Technology, 2016, 50, 1155-1166.	3.1	15
491	AOPs: recent advances to overcome barriers in the treatment of water, wastewater and air. Environmental Science and Pollution Research, 2017, 24, 5987-5990.	5.3	15
492	Degradation of the cyanotoxin microcystin-LR using iron-based photocatalysts under visible light illumination. Environmental Science and Pollution Research, 2017, 24, 19435-19443.	5.3	15
493	The estrogenic proliferative effects of two alkylphenols and a preliminary mechanism exploration in MCFâ€7 breast cancer cells. Environmental Toxicology, 2020, 35, 628-638.	4.0	15
494	Nanoscale Zero-Valent Iron Confined in Anion Exchange Resins to Enhance Selective Adsorption of Phosphate from Wastewater. ACS ES&T Engineering, 2022, 2, 1454-1464.	7.6	15
495	Pervaporation separation of water–isopropanol mixtures using silicotungstic acid loaded sulfonatedpoly(ether ether ketone) composite membranes. RSC Advances, 2014, 4, 52571-52582.	3.6	14
496	Iron based sustainable greener technologies to treat cyanobacteria and microcystin-LR in water. Water Science and Technology: Water Supply, 2017, 17, 107-114.	2.1	14
497	Microbially reduced humic acid promotes the anaerobic photodegradation of 17αÂ-ethinylestradiol. Ecotoxicology and Environmental Safety, 2019, 171, 313-320.	6.0	14
498	Black phosphorous-based nanostructures in environmental remediation: Current status and future perspectives. Chemical Engineering Journal, 2020, 389, 123460.	12.7	14
499	Quercetin exerts bidirectional regulation effects on the efficacy of tamoxifen in estrogen receptorâ€positive breast cancer therapy: An in vitro study. Environmental Toxicology, 2020, 35, 1179-1193.	4.0	14
500	A novel rutile TiO2/AlPO4 core-shell pigment with substantially suppressed photoactivity and enhanced dispersion stability. Powder Technology, 2020, 366, 537-545.	4.2	14
501	Fabrication of Bi1.81MnNbO6.72/sulfite system for efficient degradation of chlortetracycline. Chemosphere, 2021, 268, 129269.	8.2	14
502	Advanced oxidation processes for the treatment of contaminants of emerging concern. , 2020, , 299-365.		13
503	Influence of catalyst zeta potential on the activation of persulfate. Chemical Communications, 2021, 57, 7814-7817.	4.1	13
504	Removal of humic acid and Cr(â¥) from water using ZnO–30N-zeolite. Chemosphere, 2021, 279, 130491.	8.2	13

#	Article	IF	CITATIONS
505	Reactivity and reaction mechanisms of sulfate radicals with lindane: An experimental and theoretical study. Environmental Research, 2021, 201, 111523.	7.5	13
506	Nonradical Activation of Peroxydisulfate with In Situ Generated Amorphous MnO ₂ in an Electro-Permanganate Process: Involvement of Singlet Oxygen, Electron Transfer, and Mn(III) _{aq} . ACS ES&T Engineering, 2022, 2, 1316-1325.	7.6	13
507	Inference of emission history of neonicotinoid pesticides from marine sediment cores impacted by riverine runoff of a developed agricultural region: The Pearl River Basin, China. Water Research, 2022, 218, 118475.	11.3	13
508	Prediction of key structural features responsible for aromaticity of single-benzene ring pollutants and their photooxidative intermediates. Chemical Engineering Journal, 2015, 276, 261-273.	12.7	12
509	Characterization of an aerosol microconcentrator for analysis using microscale optical spectroscopies. Journal of Aerosol Science, 2017, 104, 66-78.	3.8	12
510	Enhanced CO2 photoconversion activity of TiO2 via double effect of CoPi as hole traps and high CO2 capture. Catalysis Today, 2020, 340, 204-208.	4.4	12
511	Optical characteristics and cytotoxicity of dissolved organic matter in the effluent and sludge from typical sewage treatment processes. Science of the Total Environment, 2020, 725, 138381.	8.0	12
512	Enhanced photocatalytic oxidizing ability of Zn1-xln2x/3S solid solution via band structure by composition regulation. Separation and Purification Technology, 2021, 255, 117726.	7.9	12
513	Transport and Fate of Virus-Laden Particles in a Supermarket: Recommendations for Risk Reduction of COVID-19 Spreading. Journal of Environmental Engineering, ASCE, 2021, 147, .	1.4	12
514	Nanostructured Titanium Oxide Film- and Membrane-Based Photocatalysis for Water Treatment. , 2009, , 39-46.		11
515	Spectroscopic study on interaction between three cationic surfactants with different alkyl chain lengths and DNA. Spectrochimica Acta - Part A: Molecular and Biomolecular Spectroscopy, 2015, 151, 237-246.	3.9	11
516	Role of ER-α36 in breast cancer by typical xenoestrogens. Tumor Biology, 2015, 36, 7355-7364.	1.8	11
517	Solubilization of the macroinitiator palmitoyl modified hyperbranched polyglycerol (PHPG) in hydrocarbon fuels. Fuel, 2017, 200, 62-69.	6.4	11
518	Calibration approaches for the measurement of aerosol multielemental concentration using spark emission spectroscopy. Journal of Analytical Atomic Spectrometry, 2018, 33, 404-412.	3.0	11
519	Dissolved organic matter mediates in the anaerobic degradation of 17α-ethinylestradiol in a coupled electrochemical and biological system. Bioresource Technology, 2019, 292, 121924.	9.6	11
520	Intermittent light and microbial action of mixed endogenous source DOM affects degradation of 17β-estradiol day after day in a relatively deep natural anaerobic aqueous environment. Journal of Hazardous Materials, 2019, 369, 40-49.	12.4	11
521	Fabrication of CQDs/Bi5Nb3O15 nanocomposites for photocatalytic degradation of veterinary pharmaceutical sarafloxacin. Catalysis Today, 2020, 355, 716-726.	4.4	11
522	Editorial Overview: Emissions of Microplastics and Their Control in the Environment. Journal of Environmental Engineering, ASCE, 2021, 147, .	1.4	11

#	Article	IF	CITATIONS
523	Cationic polyacrylamide (CPAM) enhanced pressurized vertical electro-osmotic dewatering of activated sludge. Science of the Total Environment, 2022, 818, 151787.	8.0	11
524	Nanomaterials: Removal processes and beneficial applications in treatment. Journal - American Water Works Association, 2013, 105, E699.	0.3	10
525	Novel integrated carbon particle based three dimensional anodes for the electrochemical degradation of reactive dyes. RSC Advances, 2015, 5, 10799-10808.	3.6	10
526	Photocatalytic degradation of maleic anhydride using visible light-activated NF-codoped TiO2. Separation and Purification Technology, 2015, 156, 1011-1018.	7.9	10
527	Ferrites as Photocatalysts for Water Splitting and Degradation of Contaminants. ACS Symposium Series, 2016, , 79-112.	0.5	10
528	Photosensitive cellular polymeric substances accelerate 17α-ethinylestradiol photodegradation. Chemical Engineering Journal, 2020, 381, 122737.	12.7	10
529	Emerging investigator series: could the superoxide radical be implemented in decontamination processes?. Environmental Science: Water Research and Technology, 2021, 7, 1966-1970.	2.4	10
530	Simultaneous changes of exogenous dissolved organic matter treated by ozonation in properties and interaction behavior with sulfonamides. Environmental Pollution, 2021, 275, 116546.	7.5	10
531	Graphite as catalyst for UV-A LED assisted catalytic wet peroxide oxidation of ibuprofen and diclofenac. Chemical Engineering Journal Advances, 2021, 6, 100090.	5.2	10
532	Nitrogen-doped hollow carbon nanospheres as highly efficient electrocatalysts for detection of triclosan. Journal of Environmental Chemical Engineering, 2021, 9, 106022.	6.7	10
533	CHAPTER 1. Photocatalytic Degradation of Organic Contaminants in Water: Process Optimization and Degradation Pathways. RSC Energy and Environment Series, 2016, , 1-34.	0.5	10
534	Low concentrations of 17βâ€estradiol exacerbate tamoxifen resistance in breast cancer treatment through membrane estrogen receptorâ€mediated signaling pathways. Environmental Toxicology, 2022, 37, 514-526.	4.0	10
535	Dissolved oxygen inhibits the promotion of chlorothalonil photodegradation mediated by humic acid. Journal of Photochemistry and Photobiology A: Chemistry, 2018, 360, 289-297.	3.9	9
536	Ultrathin and coiled carbon nanosheets as Pt carriers for high and stable electrocatalytic performance. Applied Catalysis B: Environmental, 2020, 269, 118764.	20.2	9
537	Insight into enhanced Fenton-like degradation of antibiotics over CuFeO2 based nanocomposite: To improve the utilization efficiency of OH/O2- via minimizing its migration distance. Chemosphere, 2022, 294, 133743.	8.2	9
538	Reconsidering the use of ferrous hydroxide for remediation of chlorinated ethylene contaminated groundwater: Ultra-fast trichloroethene dechlorination by ferrous hydroxide and bone char mixture. Chemical Engineering Journal, 2022, 438, 135516.	12.7	9
539	Photocatalytic Degradation of a Water Soluble Herbicide by Pure and Noble Metal DepositedTiO2Nanocrystalline Films. International Journal of Photoenergy, 2008, 2008, 1-7.	2.5	8
540	Assisted activated carbonâ€microwave degradation of the sodium dodecyl benzene sulfonate by nano―or microâ€Fe ₃ O ₄ and comparison of their catalytic activity. Environmental Progress and Sustainable Energy, 2013, 32, 181-186.	2.3	8

#	Article	IF	CITATIONS
541	Mechanism for the elimination of pollutants from aqueous solutions adopting NiR2O4 (R = Fe, Cr and) Tj ETQq1 1	9:784314	f gBT /Ove
542	Purification of Dye-stuff Contained Wastewater by a Hybrid Adsorption-Periphyton Reactor (HAPR): Performance and Mechanisms. Scientific Reports, 2017, 7, 9635.	3.3	8
543	Reactivation and reuse of TiO2-SnS2 composite catalyst for solar-driven water treatment. Environmental Science and Pollution Research, 2018, 25, 2538-2551.	5.3	8
544	17βâ€Estradiol inhibits testosteroneâ€induced cell proliferation in HepG2 by modulating the relative ratios of 3 estrogen receptor isoforms to the androgen receptor. Journal of Cellular Biochemistry, 2018, 119, 8659-8671.	2.6	8
545	Efficiency of Pb, Zn, Cd, and Mn Removal from Karst Water by Eichhornia crassipes. International Journal of Environmental Research and Public Health, 2020, 17, 5329.	2.6	8
546	Removal of As(III) from Water Using the Adsorptive and Photocatalytic Properties of Humic Acid-Coated Magnetite Nanoparticles. Nanomaterials, 2020, 10, 1604.	4.1	8
547	Designing NAZO@BC electrodes for enhanced elimination of hydrophilic organic pollutants in heterogeneous electro-Fenton system: Insights into the detoxification mediated by 1O2 and •OH. Journal of Hazardous Materials, 2022, 431, 128598.	12.4	8
548	Novel Photocatalysts for Environmental and Energy Applications. Catalysts, 2022, 12, 458.	3.5	8
549	Iron-Based Nanomaterials for the Treatment of Emerging Environmental Contaminants. ACS Symposium Series, 2013, , 135-146.	0.5	7
550	17β-estradiol at low concentrations attenuates the efficacy of tamoxifen in breast cancer therapy. Environmental Pollution, 2019, 255, 113228.	7.5	7
551	Zinc oxide-coated zeolite adsorbs and inactivates waterborne Staphylococcus aureus. Chemosphere, 2019, 229, 1-7.	8.2	7
552	Sensitive Electrochemical Detection of Microcystin-LR in Water Samples Via Target-Induced Displacement of Aptamer Associated [Ru(NH ₃) ₆] ³⁺ . ACS ES&T Engineering, 2021, 1, 1597-1605.	7.6	7
553	Opportunities for Treatment and Reuse of Agricultural Drainage in the United States. ACS ES&T Engineering, 2022, 2, 292-305.	7.6	7
554	New insight to superoxide radical-mediated degradation of pentachlorophenate: Kinetic determination and theoretical calculations. Chemical Communications, 2022, , .	4.1	7
555	Nano-enhanced treatment of per-fluorinated and poly-fluorinated alkyl substances (PFAS). Current Opinion in Chemical Engineering, 2022, 35, 100779.	7.8	7
556	Technology Baselines and Innovation Priorities for Securing Water Supply. ACS ES&T Engineering, 2022, 2, 271-272.	7.6	7
557	Understanding mechanism of improved-dewatering of waste activated sludge by multi-stage pressurized vertical electro-osmotic. Chemical Engineering Research and Design, 2022, 164, 846-856.	5.6	7
558	Room Temperature Ionic Liquids as Solvent Media for the Photolytic Degradation of Environmentally Important Organic Contaminants. ACS Symposium Series, 2005, , 182-198.	0.5	6

#	Article	IF	CITATIONS
559	Nanostructured Titanium Oxide Film- and Membrane-Based Photocatalysis for Water Treatment. , 2014, , 123-132.		6
560	Spontaneous changes in dissolved organic matter affect the bio-removal of steroid estrogens. Science of the Total Environment, 2019, 689, 616-624.	8.0	6
561	Future Trends in Photocatalysis for Environmental Applications. Journal of Hazardous Materials, 2019, 372, 1-2.	12.4	6
562	Selective spectrophotometric determination of peroxydisulfate based on a by-product formation. Sensors and Actuators B: Chemical, 2021, 344, 130214.	7.8	6
563	Treatment of contaminants of emerging concern and pathogens using electrophotocatalytic processes: A review. Current Opinion in Green and Sustainable Chemistry, 2021, 32, 100527.	5.9	6
564	Rapid detoxification of dioxin and simultaneous stabilization of targeted heavy metals: New insight into a microwave-induced pyrolysis of fly ash. Chemical Engineering Journal, 2022, 429, 131939.	12.7	6
565	The photodegradation of 17 alpha-ethinylestradiol in water containing iron and dissolved organic matter. Science of the Total Environment, 2022, 814, 152516.	8.0	6
566	The Development and Challenges of Oxidative Abatement for Contaminants of Emerging Concern. , 2020, , 131-152.		5
567	CHAPTER 8. Self-Cleaning Photocatalytic Activity: Materials and Applications. RSC Energy and Environment Series, 2016, , 204-235.	0.5	5
568	Novel strategy for enhanced visible light-responsive photoactivity of ZnFe2O4 with a single-mode microwave combustion process: Primary parameters. Chemical Engineering Journal, 2022, 440, 135551.	12.7	5
569	Kinetics and mechanistic aspects of superoxide radical-mediated transformation of ascorbate. Journal of Environmental Chemical Engineering, 2022, 10, 107736.	6.7	5
570	The path towards healthier societies, environments, and economies: a broader perspective for sustainable engineered nanomaterials. Clean Technologies and Environmental Policy, 2016, 18, 2279-2291.	4.1	4
571	Novel slow release ammonium persulfate capsules for in situ remediation of high arsenic groundwater. Journal of Hydrology, 2021, 600, 126571.	5.4	4
572	Photodegradation of 17α-ethynylestradiol in nitrate aqueous solutions. Environmental Engineering Research, 2016, 21, 188-195.	2.5	4
573	Quantitative assessment on the contribution of direct photolysis and radical oxidation in photochemical degradation of 4-chlorophenol and oxytetracycline. Environmental Science and Pollution Research, 2016, 23, 14307-14315.	5.3	3
574	Corrigendum to "Degradation of 1,4-dioxane from industrial wastewater by solar photocatalysis using immobilized NF-TiO2 composite with monodisperse TiO2 nanoparticles―[Appl. Catal. B: Environ. 180 (2016) 44–52]. Applied Catalysis B: Environmental, 2016, 196, 232.	20.2	3
575	Organic and nitrogen load removal from bio-treated landfill leachates by a dual-anode system. Environmental Science: Water Research and Technology, 2018, 4, 2104-2112.	2.4	3
576	The rapidly growing role of UV-AOPs in the production of safe drinking water. Environmental Science: Water Research and Technology, 2018, 4, 1211-1212.	2.4	3

#	Article	IF	CITATIONS
577	Silver Nanoparticle Interactions with Surfactant-Based Household Surface Cleaners. Environmental Engineering Science, 2021, 38, 481-488.	1.6	3
578	In-situ mediation of graphitic carbon film-encapsulated tungsten carbide for enhancing hydrogen evolution performance and stability. Electrochimica Acta, 2021, 388, 138566.	5.2	3
579	Mechanisms through which reductants influence the catalytic performance of a pyrophosphate-modified Fenton-like process under circumneutral pH conditions. Chemical Engineering Journal, 2022, 435, 133003.	12.7	3
580	Efficient synergism of K2FeO4 preoxidation/ MIEX adsorption in ultrafiltration membrane fouling control and mechanisms. Journal of Membrane Science, 2022, 648, 120331.	8.2	3
581	Removing Steroids from Contaminated Waters Using Radical Reactions. ACS Symposium Series, 2010, , 213-225.	0.5	2
582	Solar Water Disinfection Using NF-codoped TiO2 Photocatalysis: Estimation of Scaling-up Parameters. International Journal of Chemical Reactor Engineering, 2013, 11, 701-708.	1.1	2
583	Nanomaterials Synthesis, Applications, and Toxicity 2012. Journal of Nanotechnology, 2013, 2013, 1-2.	3.4	2
584	A System-of-Systems Framework for Improved Human, Ecologic and Economic Well-Being. Sustainability, 2017, 9, 616.	3.2	2
585	Graphitic materials in photo(electro)catalysis. Catalysis Today, 2018, 315, 1.	4.4	2
586	Multivariate calibration for carbon nanotubes in the environment using the microwave induced heating method. Environmental Nanotechnology, Monitoring and Management, 2019, 11, 100204.	2.9	2
587	Template-mediated growth of tungsten oxide with different morphologies for electrochemical application. Materials Letters, 2020, 264, 127309.	2.6	2
588	Photocatalytic Assessment of Selective Distribution of Product Arising from Methanol Oxidation on Platinum-deposited TiO2 Mesoporous Layer in a Fixed-film UV Reactor. Journal of Photochemistry and Photobiology A: Chemistry, 2020, 403, 112868.	3.9	2
589	Dataset of the efficiency of the ultraviolet light activation of persulfate ion for the degradation of cobalt cyanocomplexes in synthetic mining wastewater. Data in Brief, 2020, 29, 105346.	1.0	2
590	Response to Comment on "Mechanistic Understanding of Superoxide Radical-Mediated Degradation of Perfluorocarboxylic Acidsâ€: Environmental Science & Technology, 2022, 56, 5289-5291.	10.0	2
591	Chemically Induced Redox Reactions in Water Treatment: A Summary of Advanced and Direct Technologies. , 2006, , 1.		1
592	Enhancement of the Photodegradation of Methylene Blue by Combined Titania Photocatalyst and Photo-Fenton. Journal of Advanced Oxidation Technologies, 2008, 11, .	0.5	1
593	Degradation of atrazine in the electrochemical LED-UV/Cl ₂ system: the role of ˙OH and Cl˙. Environmental Science: Water Research and Technology, 2021, 7, 1630-1642.	2.4	1
594	Graphitic Carbon Nitride Platforms Modified with Gold-Aryl Nanoparticles for Efficient Electrocatalytic Hydrogen Evolution. Comments on Inorganic Chemistry, 0, , 1-22.	5.2	1

#	Article	IF	CITATIONS
595	Commemorative Issue in Honor of Professor Gerhard Ertl on the Occasion of His 85th Birthday. Catalysts, 2022, 12, 624.	3.5	1
596	Linking the Physicochemical Properties of Calcined Titania Nanoparticles with Their Biocidal Activity. Inventions, 2016, 1, 26.	2.5	0
597	The common, different and unique effects of metallic engineered nanomaterials: an analytic perspective. Clean Technologies and Environmental Policy, 2017, 19, 1487-1507.	4.1	0
598	Rapid and versatile pre-treatment for quantification of multi-walled carbon nanotubes in the environment using microwave-induced heating. Environmental Science and Pollution Research, 2019, 26, 13999-14012.	5.3	0
599	Modeling of Photooxidative Degradation of Aromatics in Water Matrix: A Quantitative Structureâ ''Property Relationship Approach. ACS Symposium Series, 2019, , 257-292.	0.5	0